applied sciences

MDPI

Review

Electrospinning of High-Performance Nanofibres: State of the Art and Insights into the Path Forward

Jemma R. P. Forgie [1], Floriane Leclinche [2], Emilie Dréan [2] and Patricia I. Dolez [1,*]

[1] Department of Human Ecology, University of Alberta, Edmonton, AB T6G 2R3, Canada
[2] Laboratory of Textile Physics and Mechanics, University of Haute-Alsace, 68093 Mulhouse, France
* Correspondence: pdolez@ualberta.ca

Abstract: Nanofibrous membranes have gained interest for their small pore size, light weight, and excellent filtration. When produced from high-performance polymers, nanofibrous membranes also benefit from excellent mechanical properties, thermal resistance, and chemical resistance. Electrospinning is a common method of producing high-performance nanofibres. However, there are still major challenges with the dissolution and electrospinning of these polymers, as well as in the performance of the resulting nanofibres, which is often less than what would be expected from a conventional high-performance fibre. This review assesses the state of progress in the electrospinning of five high-performance fibres: meta-aramid (m-aramid), para-aramid (p-aramid), polyamide-imide (PAI), polybenzoxazole (PBO), and polybenzimidazole (PBI). Polymers that can be readily dissolved in organic solvents, such as m-aramid, PAI, and PBI, have been more widely researched for electrospinning compared to those that can only be spun from precursors or dissolved in non-volatile solvents. Major focuses within the literature include optimizing the electrospinning process and improving the mechanical performance of the nanofibres. This review demonstrates a clear need for more standardized characterization methods and consideration for the longevity of the nanofibrous membranes. Future research should also focus on scale-up methods of electrospinning so that the benefits of nanofibres made from high-performance polymers can be leveraged by the industry.

Keywords: electrospinning; high-performance fibres; nanofibre

check for updates

Citation: Forgie, J.R.P.; Leclinche, F.; Dréan, E.; Dolez, P.I. Electrospinning of High-Performance Nanofibres: State of the Art and Insights into the Path Forward. *Appl. Sci.* **2023**, *13*, 12476. https://doi.org/10.3390/app132212476

Academic Editors: Chaoqun Dong and Xiaoming Tao

Received: 18 October 2023
Revised: 14 November 2023
Accepted: 16 November 2023
Published: 18 November 2023

Copyright: © 2023 by the authors. Licensee MDPI, Basel, Switzerland. This article is an open access article distributed under the terms and conditions of the Creative Commons Attribution (CC BY) license (https://creativecommons.org/licenses/by/4.0/).

1. Introduction

High-performance fibres show enhanced properties compared to conventional fibres including excellent mechanical properties, flame resistance, thermal resistance, and chemical resistance [1]. As demands for stronger, safer, lighter, and faster textiles increase, so too do the demands for high-performance fibres. Today, these fibres are employed for a variety of applications including aerospace, biomedical, construction, protective clothing, geotextiles, and electronics. High-performance polymers can also be used to produce nanofibres, allowing the polymers' properties to be combined with the benefits of nanoscale materials including light weight, high surface area to volume ratio, and morphology variation to achieve unique material properties [2]. Nanofibres are one-dimensional nanomaterials with diameters in the nanoscale [3]. Nanofibrous membranes have been used in a wide variety of applications including biomedical and tissue engineering, energy storage, electronics, filtration, and protective clothing [2,4]. The use of high-performance polymers to produce nanofibres provides a means to improve the mechanical, thermal, and chemical properties of the nanofibrous membranes [3].

A variety of methods can be used to produce nanofibres [4]. Bottom-up methods rely on a high degree of precision but can create unique and hyper-specific morphologies by combining polymeric building blocks. Top-down methods require less precision, thus limiting their customizability, but allow for the continuous production of a nanofibrous web. This is advantageous for industrial scale-up, as nanofibres can be more readily

mass-produced using top-down methods. The most popular method of production for nanofibres is electrospinning. In electrospinning, high voltage in the kV range is used to form a liquid jet from a polymer melt or solution. This jet becomes solidified as the melt is frozen or the polymer solution is evaporated and is then deposited on a collector, creating a nanofibrous membrane structure. The process is highly adaptable, and a wide variety of materials including polymers, metals, and ceramics can be used to produce nanofibres via electrospinning. Fibre morphologies may be adapted to create porous fibres [5], helical fibres [6], and composite fibres [7]. The collectors can be varied to alter the resultant fibre output, producing randomly oriented membranes, highly aligned membranes, uniquely designed structures, and nanofibrous yarns [4]. Electrospinning is a scalable, repeatable, convenient process with great versatility to produce a number of fibre morphologies, which makes it the most popular nanofibre production method today [2].

For high-performance polymers, electrospinning has been used to produce nanofibres from polymers including m-aramid [7–12], p-aramid [3,13–15], PAI [5,16–21], PBO [16,22–25], and PBI [26–33]. Although some reviews have considered high-performance nanofibre fabrication for specific applications [34,35], or a specific type of high-performance fibre [14,36], no reviews so far have summarized the general progress in the electrospinning of high-performance nanofibres. An enhanced understanding of the challenges and progress in fabrication techniques among high-performance fibres is a necessary step in working toward the wider adoption and mass production of high-performance fibres. Since electrospinning currently provides the most scalable method for producing nanofibrous membranes, this method of nanofabrication will be the focus of the review. The progress and challenges in the electrospinning of high-performance fibres will be discussed here to provide a summary of the field and determine the critical next steps in the advancement of electrospun high-performance fibres.

2. Electrospinning

Electrospinning is an efficient and scalable method of producing nanofibres with diameters between 40 and 2000 nm [37]. In its most basic form, the electrospinning setup consists of a high-voltage power supply, a needle spinneret, and a grounded collector [38]. The high-voltage power supply is attached to the spinneret and the conductor to create an electric field between the two elements. The spinneret supplies the polymer solution at a fixed rate. As free charges within the base of the polymer solution interact with the electric field, force is transferred to the solution [37]. This interaction forms the jet, where the polymeric solution stretches because of its interaction with the electric field, forming fibres. The jet stretches as it moves toward the collector, causing a decrease in diameter and an increase in length. Splaying occurs when external forces overcome the cohesive force of the jet, causing the jet to break up into many smaller branches. This encourages more stretching and the evaporation of the solvent. Finally, the jet is stopped at the point of the collector, where fibres are collected onto a substrate. For polymer solutions made with volatile solvents, the fibres can be deposited directly onto a collector and form a nonwoven membrane throughout the electrospinning process. Stationary collectors allow for the random deposition of fibres, creating a porous structure that shares similar mechanical properties in both the longitudinal and transverse directions [38]. In contrast, rotating collectors encourage the alignment of nanofibres, producing a membrane with enhanced strength in the longitudinal direction. The degree of alignment may be adjusted through the speed of collector rotation. Increasing the speed of drum rotation will encourage the fibres to become highly aligned. For solutions that use non-volatile solvents, a coagulating bath may be used as a collector to remove the excess solvent and form fibres [37].

The successful formation and stretching of a polymer jet to produce nanofibres requires the manipulation of many elements toward coherence. A basic overview of the parameters impacting the electrospinning process is shown in Figure 1. Firstly, the properties of the solution should be adjusted in order to achieve the optimal stretching of the jet [39]. The polymer must be soluble enough to be dissolved in a solvent at an adequate concentration.

The concentration may vary depending on the polymer but generally must be high enough to achieve sufficient polymer entanglement. Polymer chains that are highly entangled will result in a more viscous solution than polymer chains that are shorter and dispersed throughout the solution. If the solution viscosity is too low, then the stretching of the jet will not occur, and electrospraying may occur instead of electrospinning. However, if the viscosity is too high, the solution may clog the spinneret, inhibiting electrospinning. Therefore, having an appropriate viscosity is vital to the electrospinning process. In polymer science, viscosity is typically measured via intrinsic viscosity, which relates the viscosity of the solution to the molecular weight and the shape of the polymer (Equation (1)) [2].

$$[\eta] = KM^a, \tag{1}$$

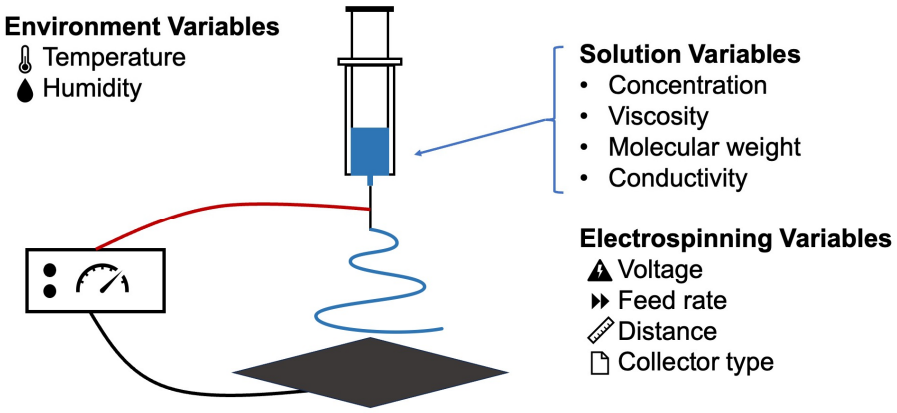


Figure 1. Basic electrospinning process and variables.

In Equation (1), $[\eta]$ is the intrinsic viscosity, K is a constant, M is the molecular weight of the polymer, and a is a function of the polymer coil shape. Therefore, an increase in molecular weight will increase the intrinsic viscosity. Further, an uncoiled or relaxed polymer chain is associated with an increased intrinsic viscosity, while a curled polymer chain is associated with a decrease in viscosity.

The choice of solvent can have a major impact on the configuration of the polymer, with a 'good' solvent allowing the polymer to fully relax within the solution, and a 'bad' solvent causing the polymer to adopt a curled configuration [2]. A good solvent will typically dissolve a greater concentration of polymer before reaching a gelation state. This encourages greater polymer–polymer contact and thus an increased solution viscosity. Therefore, choosing a suitable solvent for the polymer is necessary to produce an appropriate viscosity for electrospinning. The initial formation of the jet also relies on electrostatic force overcoming the surface tension of the solution, thus a balance between surface tension and applied voltage is necessary to maintain stability. If the surface tension is too high, the jet will not be able to maintain stability and beads will form within the jet. Finally, the solution should be sufficiently conductive to carry charges that can assist in stretching the jet and overcoming the surface tension.

The parameters of the electrospinning setup must also be optimized for the successful formation of homogenous fibres [38]. The formation of a jet relies on a voltage that is greater than the critical voltage (V_C). This is the voltage at which the surface tension is overcome and repulsive forces begin to stretch the jet. The Vc can be calculated according to the Taylor calculation [38,40]:

$$V_C^2 = 4\frac{H^2}{h^2}\left(ln\left(\frac{2h}{R}\right) - 1.5\right)(1.3\pi R\gamma)(0.09) \tag{2}$$

where H is the distance between the spinneret and collector, h is the length of the liquid column, R is the inner radius of the needle or spinneret, and γ is the surface tension of the spinning solution. Below this voltage, electrospinning will not occur. Above V_C, there is

a voltage range that will allow the formation of stable and continuous nanofibres. As the voltage increases, the jet accelerates, moving the solution from the tip of the needle to the collector faster. If the voltage is too high, the base of the jet becomes unstable and may recede into the spinneret. However, the effects of voltage on nanofibre diameter are still unclear. An increase in voltage can encourage the jet to stretch, resulting in finer fibres. However, it also accelerates the speed of the jet, which causes the fibres to move toward the collector more quickly, resulting in larger fibre diameters. As the voltage affects the electrical field, so too does the distance between the spinneret and collector.

The distance between the tip of the spinneret and the collector can be adjusted to manipulate the electric field strength and the acceleration of the jet [38]. When the distance is small, the electric field becomes stronger, and the acceleration of the jet is high. This can result in fibres with larger diameters and residual solvent, as there is little time for the jet to stretch and for the solvent to evaporate. At a larger distance, there is more time for the jet to stretch, thus thinner fibres may form. However, increasing the distance too much may lead to thicker fibres due to a weakened electric field strength. Furthermore, the flow rate determines the amount of polymer solution that is exposed to the electric field and drawn into the jet at a given time. Although it is thought that the flow rate has a lower impact on the electrospinning process, it must still be optimized to avoid interruptions in electrospinning or the formation of beads.

Finally, the ambient temperature and humidity should be considered to achieve the desired fibre morphology. An increase in ambient temperature can cause a decrease in the viscosity of the polymer solution, which may result in an increase in fibre diameter [41]. Low humidity can increase the rate of solvent evaporation, potentially leading to roughness in fibre diameters. High humidity may result in water droplets from the air condensing onto the jet, creating a porous fibre structure [38]. High humidity can also cause the discharge of electricity into the air, posing a potential safety hazard.

Although electrospinning is a relatively simple and inexpensive process to perform, there are many factors that can impact the resultant fibre diameter. As a result, large deviations in electrospinning parameters between studies dealing with the same polymers are often observed [42]. The use of different electrospinning setups, solution properties, spinneret types, and collector types can greatly affect the resultant nanofibres.

3. Electrospinning of High-Performance Polymers

Within the category of high-performance polymers, this review considers lyotropic liquid crystalline polymers (m-aramid, p-aramid, and PAI) and heterocyclic rigid-rod polymers (PBO and PBI) [1]. These polymers are among the most-used high-performance fibres and have generated interest in electrospinning research. They share common qualities including excellent mechanical properties, chemical resistance, thermal resistance, and flame resistance. As a result, these high-performance polymers are interesting candidates for applications where improved durability, chemical resistance, and/or thermal resistance are required by a nanofibrous membrane. In the next sections, the current state of the literature is discussed with respect to each fibre type.

3.1. Meta-Aramid

Meta-aramid (m-aramid) fibres are composed of poly(m-phenyleneisophthalamide) and were the first aramid fibres to be released onto the market [1]. Today, there are two commercial versions of m-aramid fibres: Nomex® from DuPont and Conex® from Teijin. Kermel® fibre, commercialized by Rhodia, is sometimes classified as an m-aramid fibre, but its structure is different, which affects its electrospinning process; therefore, it is covered in a separate section (Section 3.2). The structure of m-aramid is aromatic, containing a large number of double bonds and high C/H ratios [1]. This provides the polymer with inherent flame resistance. M-aramid is also highly temperature resistant. The polymer maintains its useful properties up to 370 °C and displays self-extinguishing properties upon ignition. As a result, m-aramid nanofibres are a popular choice in applications where flame resistance

is required for a nanofibrous membrane. For example, Merighi et al. [43] studied the use of m-aramid nanowebs to act as a wood-surface flame retardant. Other applications of m-aramid nanofibres include antimicrobial water filters [8], lithium-ion batteries [7], and breathable waterproof membranes [21].

Multiple studies have confirmed the feasibility of electrospinning m-aramid. M-aramid is readily soluble in many polar aprotic solvents including dimethylacetamide (DMAc), dimethylformamide (DMF), dimethyl sulfoxide (DMSO), and N-methyl-2-pyrroidone (NMP) [11]. However, due to the highly crystalline structure of the polymer, the use of solvent alone can only swell the polymer. To fully relax and dissolve m-aramid, the solvent is combined with alkaline salts such as lithium chloride and calcium chloride. In this process, the lithium and calcium ions link to the carbonyl group in the solvent, leaving the chloride ions free to interact with the m-aramid polymers. These ionic interactions allow for improved solubility of the polymer in the solvent. DMAc and LiCl is the most common solvent system reported for m-aramid polymers and was found to be the best solvent system for producing m-aramid nanofibrous webs with good mechanical properties (e.g., Figure 2) [11]. NMP is also an effective solvent for dissolving m-aramid with both LiCl and $CaCl_2$, but the solvent properties made electrospinning difficult. Notably, DMF and DMSO are less effective at dissolving m-aramid. Both solvents require high concentrations of salt to fully dissolve m-aramid at a 10 wt% concentration. The addition of salt changes the viscosity and conductivity of the solution, which impacts the diameter of the resultant nanofibres. With an increase in the concentration of LiCl salts, the average fibre diameter increases [11]. Generally, optimal concentrations of LiCl range from 0.5 wt% to 4 wt% for solutions containing between 10 wt% and 14 wt% m-aramid [11,43]. As a starting point to produce m-aramid polymer solutions, a variety of polymer sources were used. In many cases, m-aramid polymer (presumably in powdered form) was purchased directly for use [7,9,12,21,43,44]. However, there were instances in which m-aramid fibres were used as a polymer source for the solution [8,11,45–47]. Moreover, some studies chose to synthesize their own m-aramid prior to electrospinning [48,49].

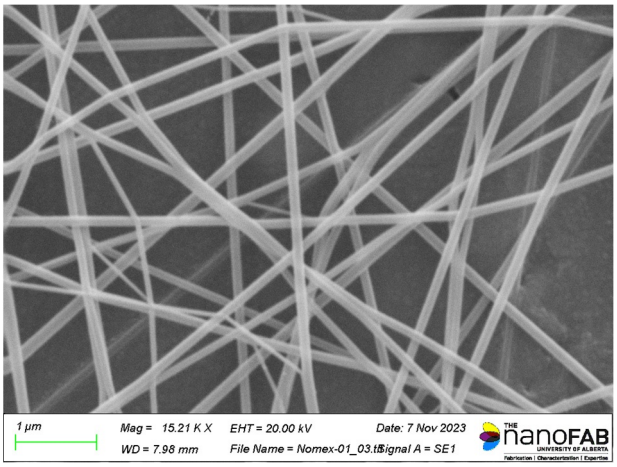


Figure 2. SEM Image of m-aramid nanofibres spun from a solution of 14 wt% Nomex and 3 wt% LiCl in DMAc. The electrospinning parameters are a voltage of 11 kV, a distance of 20 cm, and a flow rate of 0.025 mL/h. The nanofibre diameter is in the range of 105–155 nm.

Although m-aramid has been electrospun by many different researchers, the exact parameters for electrospinning have varied widely between individual studies. Table 1 describes some of the different electrospinning conditions for producing m-aramid nanofibres. Voltage is one parameter that has a significant impact on fibre diameter. The electrospinning of m-aramid fibres using $CaCl_2$ and DMAc solvent at voltages of 12 kV and 15 kV produced average fibre diameters of 150 nm and 121 nm, respectively [12]; a difference of only 3 kV created a variation of 20% in the average fibre diameters. Other studies used

much higher voltages. Merighi et al. [44] found that 20–25 kV was optimal to electrospin a similar concentration of m-aramid fibres (14 wt%) with diameters of 175 nm. In most instances, optimal voltages for electrospinning m-aramid polymers were between 15 and 25 kV [10–12,43,44]. Variations in the polymer concentration, salt type, distance, flow rate, and ambient parameters may explain similar fibre diameters reported at different voltages. Flow rates for the electrospinning of m-aramid fibres are variable, with values between 1.6 and 25 µL/min being used to supply sufficient amounts of polymer solution to the spinneret [9–12]. Distance also varied, with a maximum distance of 20 cm being used for a needle-based electrospinning setup [10].

Table 1. Electrospinning conditions of m-aramid nanofibres found in the literature.

Reference	Solution Concentration	Voltage	Distance	Flow Rate	Collector and Substrate	Temperature and Relative Humidity
[49]	14 wt% m-aramid in DMAc	15 kV	10 cm	0.05 µL/min	Rotating drum (300 rpm)	Not reported
[8]	15 wt% m-aramid and 10 wt% $CaCl_2$ in DMAc	20 kV	20 cm	1.5 mL/h	Rotating drum with aluminum foil	Not reported
[10]	9–18 wt% m-aramid in DMAc	15–25 kV	10–20 cm	0.5–1.5 mL/h	Rotating drum with stainless steel sheet	25 °C + 40%
[11]	8–14 wt% m-aramid and 1–8 wt% LiCl in DMAc	25 kV	15 cm	0.5 mL/h	Stationary collector with aluminum foil	Not reported.
[44]	14 wt% m-aramid and 4 wt% LiCl in DMAc	20–25 kV	15 cm	0.10 mL/h	Rotating drum, PE paper (60 rpm)	20–25 °C + 25%
[45]	12, 14, 16 wt% m-aramid and 5:2 ratio of m-aramid:LiCl in DMAc	15 to 20 kV	15 cm	0.2 mL/h	Rotating drum covered in aluminum foil (100 rpm)	20–25 °C + 40–50%
[12]	14 wt% m-aramid and 7.5 wt% $CaCl_2$ in DMAc	12 to 15 kV	15 cm	10 µL/min	Not reported	23 °C + 25%
[48]	8 to 16 wt% Nomex in DMAc	10–25 kV	15 cm	Not reported	Not reported	Not reported

The mechanical strength of m-aramid nanofibres has been widely investigated in the literature, for both as-spun m-aramid nanofibres and treated electrospun nanofibres. The tensile strength of m-aramid nanofibrous membranes electrospun at three different concentrations (9, 11, and 13 wt%) in a DMAc/LiCl solvent system was compared by Yao et al. [11]. It was found that the 11 wt% solution produced the nanofibrous membrane with the highest elongation at break and modulus, with a breaking strength of 1.5 mPa. At a higher concentration of 13 wt%, it was theorized that the viscosity of the solution was too high, slowing down the jet, leading to weaker conglutinated interactions among fibres. This resulted in a breaking strength of 0.25 mPa. The orientation of the nanofibres in the membrane was also found to have an effect on the overall strength of the membrane [43]. Aligning the nanofibres using a rotating collector was found to increase the elastic modulus by five times for the aligned nanofibrous mat compared to the randomly oriented mat (5000 and 1000 mPa, respectively). However, when measuring the oriented membrane in the transverse direction, the mat was so weak that it could not be properly attached to the testing frame.

Compared to conventional m-aramid fibres, initial investigations of the mechanical strength of as-spun m-aramid nanofibres found that nanofibrous membranes displayed reduced elastic modulus and strength [45]. This was attributed to a more segmented crystalline structure of the spun polymer. This lower mechanical performance limits the practical usage of electrospun m-aramid nanofibres, particularly in applications where high strength is required. One of the reasons identified for the reduced crystallinity of the as-spun nanofibrous mats is that the salts added into the polymer solution to assist with dissolution remain in the nanofibrous mats at high concentrations [45]. For example, the addition of 2 to 3.5 wt% LiCl in a solution of 14 wt% m-aramid produced a nanofibrous membrane with between 12.5 and 20 wt% LiCl [9]. The presence of this salt disrupts the formation of crystalline regions within nanofibres [9,45]. The hygroscopic nature of LiCl also leads to higher water adsorption, which can cause fibre disentanglement when the material is under tensile deformation [9]. Depending on the amount of salt, it may also increase the diameter of the nanofibres.

As a result, post-treatments of m-aramid nanofibrous membranes are being investigated to increase the crystallinity of the nanofibers and improve the mechanical properties of m-aramid nanofibrous mats. One study used a washing treatment to remove excess salt from the nanofibrous mats and improve the mechanical properties [9]. The m-aramid nanofibrous mats were washed in distilled water and dried at 70 °C. The Young's modulus increased from 170 mPa to 752 mPa after washing, confirming the significant effect of the presence of LiCl on the mechanical properties of the nanofibrous mat and showing the efficiency of the washing treatment at improving the performance of the nanofibrous mats. The annealing of m-aramid nanofibrous mats was also attempted [47]. However, a heat treatment below 200 °C showed little effect on the mechanical properties of the nanofibres. Above 200 °C, the properties of the membrane decreased. Conversely, microwave irradiation was able to remove excess solvent and salt present in the as-spun nanofibrous membrane, leading to an increase in tensile strength of 2.8 times compared to the untreated membrane [49]. However, this method was highly energy intensive. A lower-energy, solvent-assisted heat treatment was proposed as an alternative method [45]. Electrospun membranes were submersed in a solution of DMAc, water, and ethylene glycol before being heat-treated. It was found that a heat treatment of 120 °C was optimal to encourage crystallization within the nanofibres. The resultant membrane showed an increase in tensile strength and modulus compared to the untreated and heat-treated mats. The Young's modulus was 13.5 times and 1.7 times higher than that of the untreated and heat-treated membranes, respectively. It also showed improved chemical resistance. Due to the interest in m-aramid nanofibres as high-strength scaffolds for nanocomposites [7,8] and coaxial nanofibres [46], finding efficient methods to increase the crystallinity and strength of the membranes is vital in ensuring their relevance to practical applications.

Beyond optimizing the mechanical properties of m-aramid nanofibrous membranes, multiple studies have conducted other manipulations in membrane properties to make nanofibrous m-aramid mats more suitable for specific applications. One of the major advantages of working with the m-aramid polymer is its excellent resistance to heat and flame. Therefore, ensuring the heat and flame resistance of nanofibrous mats is important for many applications [10,43]. The thermal degradation of m-aramid nanofibrous mats was found to be similar to that of the corresponding staple fibre, with weight loss occurring at 100 °C due to solvent evaporation and again at 430–450 °C due to chain scission [10]. In contrast, the heat shrinkage behaviour of the m-aramid nanofibrous membranes was much larger compared to microfibrous mats. In 30 min intervals, the membrane was exposed to temperatures between 200 and 350 °C. At 200 °C, the shrinkage was 7.5%, but increasing the temperature to 350 °C resulted in a heat shrinkage of 50.4%. Work was conducted to try reducing the thermal shrinkage of m-aramid nanofibrous membranes. In one study, m-aramid/polysulfone-amide (PSA) membranes with different ratios of the two polymers were electrospun to see if the blending would improve the dimensional stability of the resulting mats after heat exposure [50]. After 200 h in a 250 °C oven, the 100% m-aramid

nanofibrous membranes had shrinkage of 10% and 6% in the warp and weft directions. In contrast, a 7/3 blend of m-aramid/PSA resulted in a 6% shrinkage in both directions, and blends of 5/5 and 3/7 displayed no shrinkage after heat exposure. PSA is a flame-resistant polymer, therefore its addition to the nanofibrous membrane should not affect the flammability of the membrane [51]. However, the flame resistance of the membrane was not tested in this study [50]. The addition of SiO_2 nanoparticles also reduced the shrinkage of the m-aramid nanofibrous membrane, providing thermal stability without shrinkage up to 260 °C [7]. Without the SiO_2, the membrane began shrinking at 260 °C. In addition, the membranes containing SiO_2 showed an increase in tensile strength compared to the pure m-aramid membranes. This is attributed to the van der Waals forces, electrostatic attraction, and polarity of the polymers and SiO_2, which may form a three-dimensional structure allowing for better dispersion of stress in the polymer and nanoparticle network. The pure m-aramid membrane had a tensile strength of 8.75 MPa, whereas the membrane containing 6 wt% SiO_2 had a strength of 18.14 MPa. However, above 6% SiO_2, the membrane strength began to decrease as the nanoparticles agglomerated within the structure.

The flame resistance of m-aramid nanofibres has also been investigated, particularly for applications as a flame-retardant coating on other materials. When m-aramid nanofibrous membranes are used to improve the flame resistance of another material, the fibre alignment and the attachment method to the material both impact the flame resistance of the system [9,43,44]. Attaching an m-aramid nanofibrous membrane to the surface of wood was found to improve its flame resistance compared to untreated wood [44]. However, it was found that randomly oriented membranes were more effective than aligned nanofibrous membranes at improving flame resistance [43]. During exposure to flame, a buildup of gases between the wood and nanofibrous membrane led to disruptions in the m-aramid layer, exposing the wood to flame. Since the randomly oriented mat had improved mechanical properties in all directions, it was more resistant to failure, thus providing better flame protection to the wood. In contrast, the aligned membrane had poor mechanical strength in the transverse direction, leading to a faster failure time. Mazzocchetti et al. [9] studied the flame resistance of m-aramid nanofibrous mats bonded to carbon fibre-reinforced composites. The presence of the nanofibrous mats did not improve the flame resistance of the material, but this behaviour was attributed to an outer layer of epoxy present on the samples, which burned before the flame reached the nanofibrous membrane. The only improvement provided by the m-aramid nanofibrous mat was the time to ignition, which increased by 50 s compared to the original carbon fibre-reinforced composite.

For liquid filtration applications, the pore size and permeability of the membrane are important in ensuring that the membrane can perform effectively. The nanofibre diameter distribution and membrane thickness are the main factors determining pore size and permeability [8,10]. In general, m-aramid nanofibrous membranes have a narrow pore size distribution compared to micro-scale fibrous filtration media, with pore sizes between 0 and 2 μm [8,10]. Pore size distribution decreases as a smaller distribution of nanofibre diameters is achieved by optimizing the concentration of m-aramid in the spinning solution [8]. Moreover, as membrane thickness increases, average pore size gradually decreases [10]. However, in m-aramid nanofibrous membranes, it was observed that pore size only decreased up to a membrane thickness of 8.95 μm, after which the pore size plateaued [10]. In general, m-aramid nanofibrous membranes perform well compared to conventional liquid filters. Liquid permeability was found to be improved in m-aramid nanofibrous membranes compared to commercial glass fibre water filters [8]. For applications for air filtration, the water vapour permeability of m-aramid was investigated for a breathable, temperature-resistant membrane [10]. The water vapour permeability was measured to be 7650 g/m^2, nearly twice the minimum value for a breathable membrane (4000 g/m^2) [52]. However, the addition of PSA used to improve the dimensional stability led to increased pore sizes and decreased mechanical strength in the nanofibrous membranes.

M-aramid nanofibrous membranes have also been adapted for specific applications. M-aramid nanofibrous membranes were investigated as a precursor to N-halamine, for

the production of an antimicrobial water filter [8]. Here, m-aramid nanofibres were submerged in a solution of diluted bleach to form an N-halamine structure. The chlorinated membrane was able to be recharged with 98% efficacy. Moreover, the membrane was able to fully remove both *Escherichia coli* and *Staphylococcus aureus* from water through a non-pressure-driven filtration process without contaminating the water with chlorine. M-aramid nanofibres were also produced with a helical morphology through co-electrospinning with an m-aramid core and thermoplastic polyurethane outer shell [46]. The production of helical nanofibres can be used in applications where high fibre resiliency is needed. M-aramid was also electrospun as a composite with SiO_2 nanoparticles in order to improve the conductivity and electrolyte uptake of the membrane [7]. The presence of SiO_2 nanoparticles increased the wettability, porosity, breaking strength, conductivity, and dimensional stability. Silver nanoparticles have also been added to m-aramid nanofibrous membranes in order to produce a high-performance flexible pressure sensor [53]. The m-aramid membrane contributed excellent mechanical and breathable properties to the sensor, making it suitable for wearable applications.

In summary, M-aramid nanofibrous membranes have been successfully produced via electrospinning using a variety of methods. The optimization of the electrospinning process through solvent, salt content, polymer concentration, and electric field behaviour has been demonstrated [9,11,46]. Moreover, methods to improve the mechanical properties and thermal stability of the nanofibres continue to improve [7,45,49,50]. M-aramid nanofibres are now being studied for specific applications, and the increasing interest in m-aramid nanofibrous composites is allowing for the enhancement of the nanofibrous membrane properties.

3.2. Polyamide-Imide

Polyamide-imide (PAI) is commercialized under the trade name Kermel® [1]. The polymer combines the properties of polyimides and polyamides, providing excellent strength and thermal stability [17]. As a result, PAI nanofibres are a popular choice in high-temperature filtration applications [19]. In electrospinning, PAI is also considered a useful alternative to polyimide, as it displays similar properties but has enhanced solubility [19]. While PI nanofibres cannot be electrospun directly, PAI may be directly dissolved in solvent and electrospun. PAI is soluble in a variety of solvents including DMAc, DMF, DMSO, pyridine, cyclohexanone, and tetrahydrofuran [54]. The electrospinning of PAI has been performed via dissolution in DMF at 25 wt% [21], in a 34 wt% NMP/DMF mixture [19], and in 1,3 dimethyl-2-imidazolidinone [20]. The use of various solvents to produce PAI solutions allows enhanced customizability of the solutions and resultant nanofibres as well as the potential for polymer blend nanofibres, as other polymers may be soluble in the same solvents.

One advantage of the excellent solubility of PAI in various solvents is that a mixed-solvent system can be used to alter the nanofibre morphology during electrospinning [19]. A mixed solvent system of NMP and DMF under high humidity produced biomimetic pine needle-like fibres with a grooved surface morphology (Figure 3). Upon exposure to high humidity, the DMF was replaced by water and formed a porous semi-solid structure. Then, the water gradually replaced the NMP, and the pores on the surface of the jet became stretched by the electrostatic repulsive forces, leading to a grooved fibre structure. The grooved structure increased the specific surface area to allow for greater adsorption and retention of particulate matter during air filtration. Electrospinning within a humid environment also led to the formation of curled fibres, which produced a highly porous membrane. Increased specific surface area and membrane porosity contributed to improved filtration and decreased pressure drop, respectively.

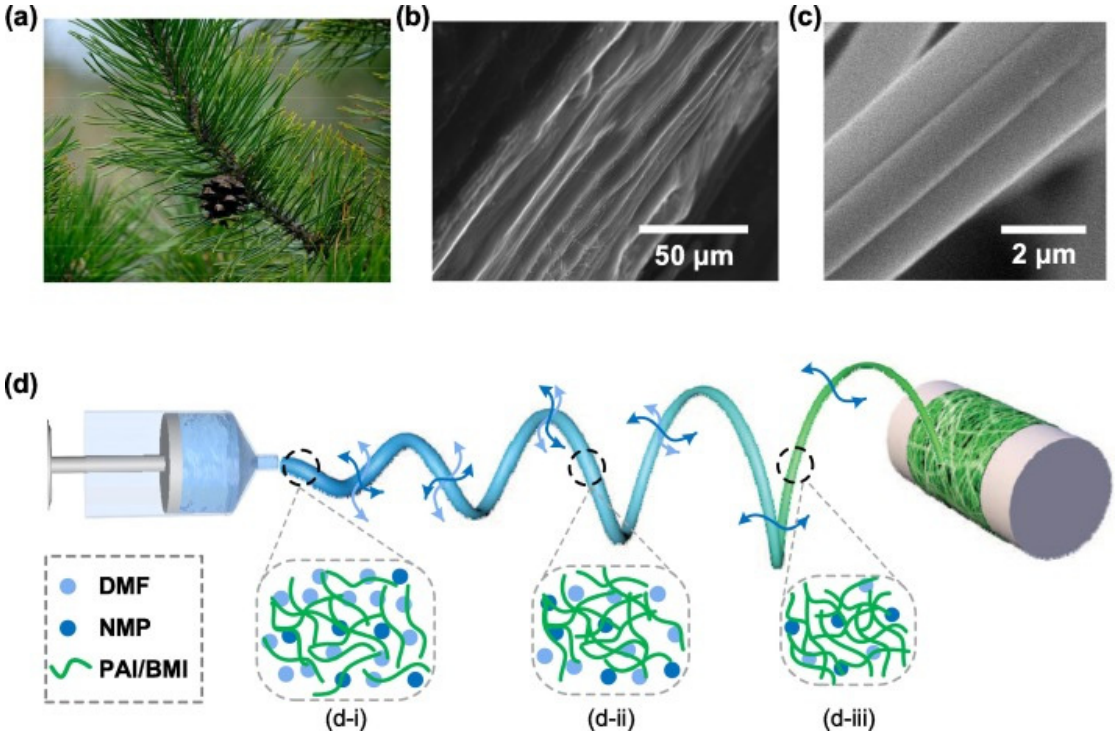


Figure 3. Biomimetic PAI nanofibres produced using a multi-solvent system. The image displays (**a**) the mason pine needles the researchers were trying to mimic, (**b**) the grooved surface of the needles under SEM, and (**c**) the grooved surface of a PAI nanofibre produced using the multi-solvent system. The schematic for producing the grooved nanofibres is shown in (**d**). Reprinted with permission from Ref. [19]. 2019, Elsevier.

PAI may also be electrospun from a precursor and then converted to PAI via post-treatment [16]. Traditionally, PAI is difficult to synthesize. However, Duan et al. [25] considered a simplified method to synthesize PAI nanofibres inspired by the two-step process for polyimide fabrication. Here, an amide-containing diamine was reacted with a dianhydride to produce a precursor solution of amide-containing polyamic acid. The precursor solution was diluted with DMAc and DMSO and electrospun at 20 kV with a distance of 25 cm and a flow rate of 0.70 mL/h. They used a disk-shaped rotating collector and a stationary collector to produce aligned and randomly oriented fibres, respectively. The membrane was then thermally treated under a nitrogen atmosphere to produce PAI. Thermal treatment was successful up to 450 °C. Above this temperature, the fibres displayed poor thermal stability. PAI nanofibres produced via electrospinning showed improved tensile strength and modulus compared to PAI films produced in the same way.

The strength of electrospun PAI nanofibres is significantly higher than that of other polymeric nanofibres including nylon, PBO, and polyimide [16]. Further improvements in the mechanical properties of PAI nanofibres may be achieved by thermal annealing at high temperatures. Aligned nanofibrous PAI membranes produced from a precursor and annealed at a temperature of 400 °C had a strength of 892 ± 15 MPa. This was a significant improvement compared to the strength of a membrane which was annealed at 350 °C, with a strength of 504 ± 4 MPa. However, further increasing the annealing temperature to 430 °C decreased the tensile strength of the nanofibrous membrane to 702 ± 6 MPa. Fibre alignment also altered the mechanical strength of the fibres, with aligned fibres showing much greater tensile strength and modulus compared to randomly aligned fibres. For example, a mat with randomly aligned nanofibres annealed at 400 °C had a strength of 120 ± 10 MPa, several times lower than the oriented nanofibrous mat.

The high strength of PAI's nanofibres also makes them an excellent candidate for reinforcement with other nanofibrous materials. PAI nanofibres have been used as a re-

inforcement in an electrospun polytetrafluoroethylene (PTFE) membrane, where it was found to significantly increase the strength of the nanofibrous membrane at a 3% concentration [17]. The PAI precursor was blended with PTFE and electrospun at a voltage of 12 kV onto a stationary collector. The membrane was then heat-treated at 380 °C for 10 min to obtain a PTFE/PAI composite. The addition of PAI was found to increase the thermal stability and strength of the nanofibrous membranes. At 20 wt% PAI, the randomly oriented membrane had a strength of 19 MPa, which was a 31% increase compared to the 100% PTFE membrane. However, the PAI led to significant changes in morphology. Where pure PTFE nanofibres showed even diameters, increasing amounts of PAI produced thinner fibres with a wider diameter distribution.

The feasibility of industrial scale-up for PAI fibres has also been examined by electrospinning PAI nanofibres on a wire-based electrospinning setup [20]. A solution of PAI was electrospun on an Elmarco Nanospider™ to determine the viability of the industrial scale-up of aramid nanofibres. While needle-based electrospinning is suitable for preliminary studies on nanofibre production, the throughput is extremely small and thus unsuitable for industrial applications. Needleless electrospinning allows for the free formation of jets across the surface of a polymer solution [55]. This allows jets to be configured optimally, leading to the most efficient spacing of jets for multi-jet electrospinning. Wire-based electrospinning is a technique patented by Elmarco; it involves a stationary wire electrode that is coated in polymer solution via a moving carriage [56]. Jets form across the surface of the wire and are distributed on a collector, which is positioned above the wire. Oertel et al. [20] used the enhanced productivity of the wire-based electrospinning setup to determine the feasibility of electrospinning PAI nanofibres at an industrial scale. A solution of PAI in 1,3-dimethyl-2-imidazolidinone is prepared with a viscosity of 60 Pa.s. Voltage, airflow, distance, relative humidity, and temperature were manipulated in order to determine the best processing parameters for PAI. It was found that relative humidity, voltage, and distance had the greatest effect on the mean fibre diameter. Relative humidity and distance were observed to have a positive effect on the mean fibre diameter. In contrast, an increase in voltage was found to slightly decrease the mean fibre diameter. Within the set parameters, increasing airflow and temperature showed no effect on the mean fibre diameter.

Finally, post-treatment of PAI has been used to increase the hydrophilicity of PAI nanofibrous mats [21]. PAI nanofibres were electrospun from a solution of PAI and DMF using a needle-based electrospinning setup. Nanofibrous membranes then underwent atmospheric-pressure plasma treatment at various times (60, 120, 180, and 240 s). Longer atmospheric-pressure plasma treatments were found to alter the chemical structure of the fibres, as well as the surface morphology. From these observations, it was found that a treatment time of 120 s was optimal to improve hydrophilicity whilst minimizing etching and oxidative reactions. Increasing the time of the atmospheric-pressure plasma treatment was found to decrease the water contact angle, but it increased again above 120 s. Therefore, it was concluded that 120 s of plasma treatment time was optimal to improve the hydrophilicity of the nanofibres.

In summary, the electrospinning of PAI has progressed into many specific applications. The ease of solubility of the polymer allows it to be readily electrospun from solution [54]. Furthermore, the cost-effective alternative to electrospinning from a precursor has also been performed for PAI [16]. A major advantage of electrospun PAI nanofibres is their high strength relative to nanofibres spun from other polymers. This makes them an excellent candidate for applications requiring high strength, as well as for reinforcement in nanofibrous membranes made from other polymers. The scale-up of PAI polymers has also been studied, with effective parameters found to produce PAI nanofibrous membranes using needleless electrospinning [20]. However, the performance characterization of membranes electrospun on the needleless setup has not been performed. Moving forward, it will be important to understand whether PAI nanofibrous membranes electrospun on a needleless setup can exhibit the same mechanical and thermal characteristics as those electrospun using a needle-based setup.

3.3. Para-Aramid

Para-aramid (p-aramid) is a class of highly crystalline high-performance fibres with superior mechanical properties and excellent chemical resistance [1]. The most popular p-aramid is poly-paraphenylene terephthalamide (PPTA), which has been commercialized by DuPont as Kevlar® and by Teijin as Twaron®. Due to its high crystallinity, the fibre is especially useful for applications requiring ballistic resistance [3]. P-aramid has high thermal resistance, with a continuous operating temperature of 190 °C and a melting temperature of 400 °C [1]. It is also inherently flame-resistant. Unfortunately, the high crystallinity and lack of sidechain groups in the p-aramid polymer make it very difficult to dissolve [3]. As a result, electrospinning from solution is very difficult to achieve. The earliest record of electrospinning p-aramid involved dissolution in a concentrated solution of sulphuric acid at a high temperature and with a grounded water bath as a collector [57]. However, this method was unable to allow a continuous electrospinning process. Moreover, the use of concentrated sulphuric acid as a solvent for p-aramid makes industrial scale-up difficult, as the solvent is corrosive.

Methods to produce p-aramid nanofibres without the use of sulphuric acid have also been explored. For the most part, p-aramid nanofibres are synthesized using alternative methods such as top-down dispersal [58], polymerization-induced self-assembly [14], and centrifugal spinning [13]. While bottom-up methods showed some promise, they still resulted in nanofibres with large diameters and low tensile strength [14]. Likewise, centrifugal spinning suffers from high energy consumption and faces the issue of equipment corrosion. Therefore, investigation into the electrospinning process is still useful. Within electrospinning, two major discoveries have encouraged the use of this method to produce p-aramid nanofibres.

Yao et al. [15] determined that anisotropic solutions of p-aramid could be more readily electrospun at higher concentrations compared to the traditional isotropic solutions (Figure 4). The p-aramid polymer was dissolved in sulphuric acid to form both isotropic p-aramid solutions at 2, 5, and 7 wt% of solid content and anisotropic solutions at 15, 17, and 19 wt%. The solution was electrospun using a needle-based electrospinning setup. Fibres were collected into a water bath for coagulation, which was necessary due to the non-volatility of sulphuric acid. A heating band was also used to maintain an electrospinning solution temperature between 80 and 90 °C. Below 80 °C, anisotropic solutions of p-aramid would begin to solidify, and above 90 °C, the solution would begin to degrade. After electrospinning, fibres had to go through an additional drying step. It was observed that the jet had minimal whipping due to high voltage and low distances (2–8 cm), which formed a very strong electric field. At lower concentrations of isotropic p-aramid solutions, only droplets were observed. At 7 wt%, some very short fibres were seen, but breakages of the solution jet prevented continuous spinning. The entanglement of the polymer at higher p-aramid concentrations in anisotropic solutions allowed for the formation of continuous fibres. However, these fibres showed large distributions in diameters, between 16 and 300 µm, which was attributed to branching during the electrospinning process. Although some nanoscale p-aramid fibres were observed, the large diameter distribution, high voltages, use of corrosive solvent, and jet breakage inhibited the continuous production of large amounts of nanofibres. Therefore, although using higher polymer concentrations in anisotropic solutions was successful in the formation of fibres via electrospinning, a continuous and scalable process could not be achieved.

Another innovation in the electrospinning of p-aramid involved the use of side-chain substitutions to improve the solubility of the polymer [3]. Through N-substitutions, the solubility of p-aramid was improved. Side-chain substitutions were performed on conventional Kevlar® (p-aramid) fibres. The side-group substitutions were confirmed with NMR. The allyl-, propyl-, and pentenyl-functionalized fibres obtained were soluble in DMAc, DMF, and NMP. Benzyl-functionalized p-aramid showed solubility in DMAc and NMP. Finally, methyl-functionalized polymers were soluble only in NMP at high temperatures. The solution was then electrospun via needle-based electrospinning onto

a stationary aluminum collector at a concentration of 20 to 50 wt%, a voltage of 20 kV, a flow rate of 0.1 mL/h, and a distance of 10 cm. In this instance, a coagulating water bath was not needed, as volatile solvents were used. Electrospinning at high voltage and low flow rate was generally successful, and fibres with an average diameter of 68 nm were produced using the propyl-functionalized p-aramid DMF at a concentration of 20 wt%. Fibre diameter was found to increase with polymer concentration, with a concentration of 50 wt% creating fibres with a diameter of 1.75 µm. This study provided a first step in the scalable and continuous electrospinning of p-aramid polymers. However, it did not fully explore the impact of the side-group substitutions on the mechanical strength of the resultant nanofibres. Since the addition of side groups can increase amorphous regions of the fibre, it is likely that this method would have a negative impact on the strength of the nanofibres.

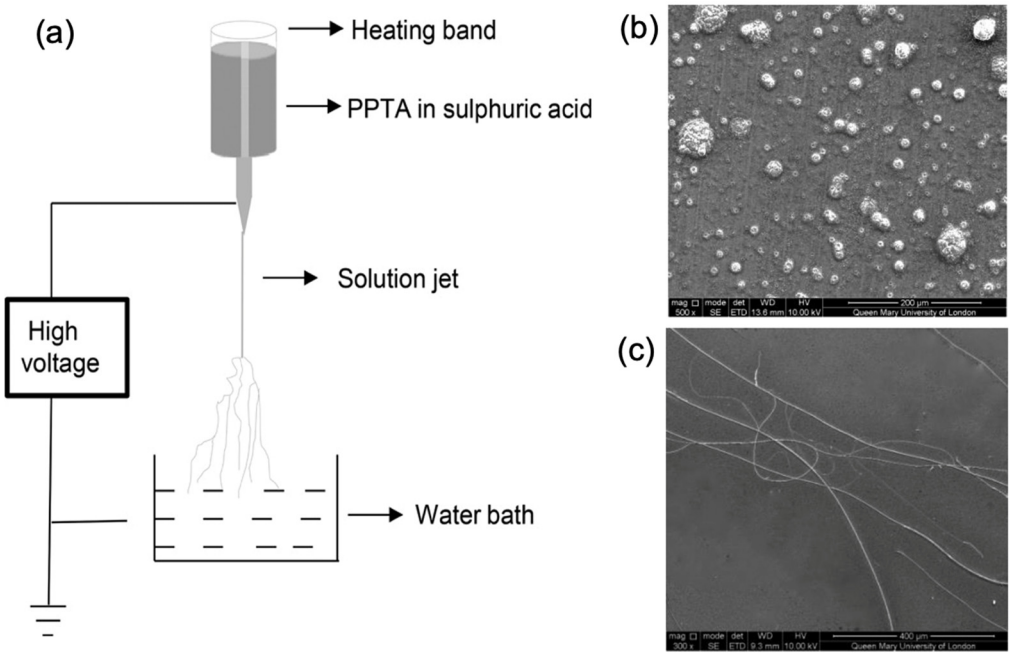


Figure 4. Electrospinning of p-aramid nanofibres in sulphuric acid: (**a**) electrospinning setup; (**b**) resulting electrospray droplets from spinning with a 4 wt% p-aramid isotropic solution; and (**c**) electrospun fibres resulting from spinning with a 19 wt% p-aramid anisotropic solution Reprinted with permission from Ref. [15]. 2015, Wiley.

In summary, compared to the electrospinning of other high-performance nanofibres, p-aramid nanofibres show considerable challenges due to the high crystallinity and low solubility of the polymer. The use of anisotropic solutions may improve the electrospinnability of the polymer but still requires the use of a highly corrosive solvent [15]. In contrast, side-chain substitutions provide a promising method to improve the electrospinning of p-aramids, as the functionalized fibres can be dissolved in common solvents [3]. Further investigation into the impacts of side-chain substitutions on the properties of the resulting nanofibrous mats will be important in determining the best applications for these. The use of post-treatments to improve the mat performance will also be a vital step to further optimize the p-aramid nanofibres.

3.4. PBO

Poly(p-phenylene-2,6-benzobisoxazole) (PBO) is a rigid-rod polymer with excellent chemical, thermal, and mechanical properties [1,59]. The conventional fibre is commercially produced by Toyobo under the trade name Zylon®. The polymer has very high thermal resistance and will not degrade in air until 600 °C [1]. PBO is also flame-resistant and has self-extinguishing properties. Although the rigid rod structure imparts many desirable

characteristics to the polymer, such as excellent mechanical properties, it also makes the processing of PBO very difficult. PBO is only soluble in strong acids, making it difficult to electrospin directly [37,59]. Instead, PBO nanofibres can be electrospun indirectly either from poly(o-hydroxy-amide)s (OH-PA) or poly(o-hydroxy-amic acid)s (OH-PAA) [25]. These precursors are soluble in organic solvents and can be transformed into PBO nanofibres via heat treatment processing after electrospinning [25,59].

The most common method of electrospinning PBO from precursors involves the electrospinning of an o-hydroxy aromatic monomer, such as poly(o-hydroxy-amide) (OH-PA) or poly(o-hydroxy-amic acid) (OH-PAA), which can be dissolved in common organic solvents, electrospun, and then thermally converted to PBO nanofibres [25]. However, using the OH-PA precursor can be problematic due to its low molecular weight, leading to poor mechanical properties of the resultant nanofibres. However, the lower molecular weight of the precursor can also lead to thinner nanofibres, which should be kept in mind while optimizing nanofibre diameters [23]. OH-PAA, having a higher molecular weight, can be used to electrospin PBO nanofibres with higher thermal resistance and improved mechanical properties. Zhang et al. [25] used a solution of 6 wt% OH-PAA in DMAc with cetyltrimethylammonium bromide (CTAB) to electrospin PBO precursor nanofibres. The solution was electrospun at 20 kV with a distance of 20 cm and collected on a rotating disc to form a nanofibre belt. The nanofibres were then heated under a nitrogen atmosphere and annealed at various temperatures to form PBO nanofibres. To assess the mechanical and thermal properties, a thermal–mechanical analyzer was used. The tensile testing of the aligned nanofibre belts was performed at various temperatures. It was observed that the modulus was well retained as the heat increased, with an 86% modulus retention at 350 °C. The test was performed up to 500 °C, where the modulus retention was still over 50%. The use of a high-molecular-weight precursor allowed for the formation of heat-resistant and high-strength PBO nanofibres with stability up to 643 °C.

However, the use of the o-hydroxy monomer as a precursor to PBO can be problematic as it is difficult to synthesize, leading to high costs that limit the scalability of the process [29,60,61]. Duan et al. [59] attempted to create PBO nanofibres using inexpensive precursor materials. Monomers of 4, 4′-diamino-3, 3′-dimethoxydiphenyl (DMOBPA), and isophthaloyl dichloride (IPC) were used in combination with DMAc, pyridinium, and LiCl to prepare a solution of methoxy-containing polyaramide (MeO-PA). The solution was electrospun on a needle-based electrospinning setup at a voltage of 30 kV, a flow rate of 0.8 mL/h, and a distance of 30 cm. The mat was then post-treated to remove LiCl and pyridinium and heat-treated under a nitrogen atmosphere. FTIR analysis indicated that a temperature of 350 °C was sufficient to transform the precursor to PBO. This method provides an inexpensive way to produce PBO nanofibres from an electrospun precursor. However, the low molecular weight of the precursor compromised the mechanical strength of the resultant nanofibres [24].

Combinations of both the high molecular weight OH-PAA and the inexpensive DMOBPA were also used to produce an affordable PBO nanofibre without compromising the mechanical strength [24]. The synthesized precursor, methoxy-containing polyamic acid (MeO-PAA), had a higher intrinsic viscosity than OH-PAA or MeO-PA and thus an increased molecular weight. MeO-PAA was electrospun onto a rotating disk collector and then heat-treated to form the ring structure of PBO. However, a direct transformation to PBO was not observed. The MeO-PAA was converted to methoxy-containing polyimide (MeO-PI) at 350 °C and to poly(imide-*co*-benzoxazole) (PI-*co*-PBO) at 450 °C and 500 °C. It is suspected that more energy is required to fully convert MeO-PI into PBO, but this was not investigated in the study. The PI-*co*-PBO nanofibres were tested for tensile strength and thermal resistance. The nanofibres demonstrated thermal resistance above 500 °C, but the thermal decomposition temperature was approximately 50 °C lower than that of PBO nanofibres directly spun from the OH-PAA precursor. The tensile strength of the PI-*co*-PBO nanofibrous belts was the highest after a heat treatment at 450 °C, which resulted in a strength of 559 MPa. Compared to the tensile strength of other high-performance films

and fibres, including m-aramid, pure PBO, and multiwalled carbon nanotubes, the tensile strength of PI-*co*-PBO was the highest that had been observed. The thermomechanical properties of the PI-*co*-PBO were slightly lower than that of the pure PBO nanofibres, with only a 76% modulus retention at 300 °C. However, the nanofibres were still sufficiently heat resistant and better maintained their strength and modulus at high temperatures when compared with other nanofibres.

In summary, the literature reflects a variety of methods to electrospin PBO from precursors, with good consideration of how each precursor type affects both the performance and scalability of the process [24,25,59]. Given the high temperature resistance and excellent mechanical properties that have been displayed by PBO nanofibres, this type of nanofibre would be suitable for several applications where high heat and durability are primary concerns. Investigations into the porosity and filtration performance of PBO, as well as the potential for composite PBO nanofibre materials, will be interesting paths forward to progress the research on PBO and determine suitable applications.

3.5. PBI

Polybenzimidazole (PBI) was developed in the 1960s; it has excellent mechanical, chemical, and thermal properties [62]. The polymer has a high glass transition temperature of 450 °C and a degradation temperature of 580 °C [1]. Due to its high thermal resistance, PBI lends itself to many applications for nanofibrous membranes. PBI nanofibrous membranes have been studied for applications including lithium-ion battery separators, fuel cells, water electrolyzers, respiratory masks, and carbon nanofibre precursors [26,28,30–32]. PBI is readily dissolved in DMAc alone and in the presence of aprotic salts such as LiCl and LiBr [26,63,64]. The earliest reported method for electrospinning PBI fibres involved a solution of 20 wt% PBI dissolved in DMAc and 4 wt% LiCl in a nitrogen atmosphere under high temperature [63]. A top-down electrospinning setup was used, where the polymer solution was contained in a glass pipette with a small opening, and the positive charge was supplied by a wire immersed directly in the polymer solution. A grounded rotating drum was used as a collector. After collection, nanofibrous mats were washed in methanol to remove excess salt and solvent, then washed again with 50% sulphuric acid to improve the thermal shrinkage resistance. Finally, the membranes were heat-treated above the glass transition temperature of PBI. This method was able to produce randomly oriented nanofibres with diameters around 260 nm. More recently, electrospun nanofibrous mats using an altered form of PBI (m-es-PBI_{net}) have been produced using needleless electrospinning on the Elmarco Nanospider [65]. The m-es-PBI_{net} was dissolved at 15 wt% in a solution of DMAc and ethanol and electrospun at a voltage of 70 kV and a distance of 180 mm. This produced nanofibres with diameters between 520 and 250 nm.

Optimizations of electrospinning processes and solution properties have been conducted for PBI nanofibres. However, there is a major focus on the application of PBI; therefore, studies looking at the effect of electrospinning parameters alone are not found in the literature. Instead, studies that examined PBI nanofibres for a specific application also performed optimization processes for the electrospinning process. Jung et al. [28] observed the impact of the PBI concentration in the polymer solution on the nanofibre diameter. PBI was dissolved in DMAc at concentrations between 14 and 18 wt% and electrospun to determine the optimal polymer concentration. At PBI concentrations of 14 and 15 wt%, highly beaded nanofibres were observed [28]. Between 16 and 18 wt%, smooth and even fibres were formed via electrospinning. It was found that 16 wt% was the optimal concentration for achieving even fibres with small diameters (90–150 nm). Higher concentrations of PBI (up to 35 wt%) have also been electrospun successfully; however, the diameter of these nanofibres was significantly higher, with a mean diameter of 729.9 nm [26]. Jahangiri et al. [27] used various solution concentrations, voltages, distances, and feed rates to optimize the electrospinning process for PBI nanofibres (Figure 5). The relationship between feed rate and polymer concentration was examined; it was determined that 15 wt% PBI and 100 µL/h was the most effective combination for stable electrospinning and bead-free fibres

with an average diameter of 170 nm. The effects of voltage were also characterized using voltages of 12, 15, and 18 kV. It was found that the combination of 15 wt% PBI, 15 kV, and 100 µL/h was the most effective for a reproducible electrospinning process with smaller fibre diameters.

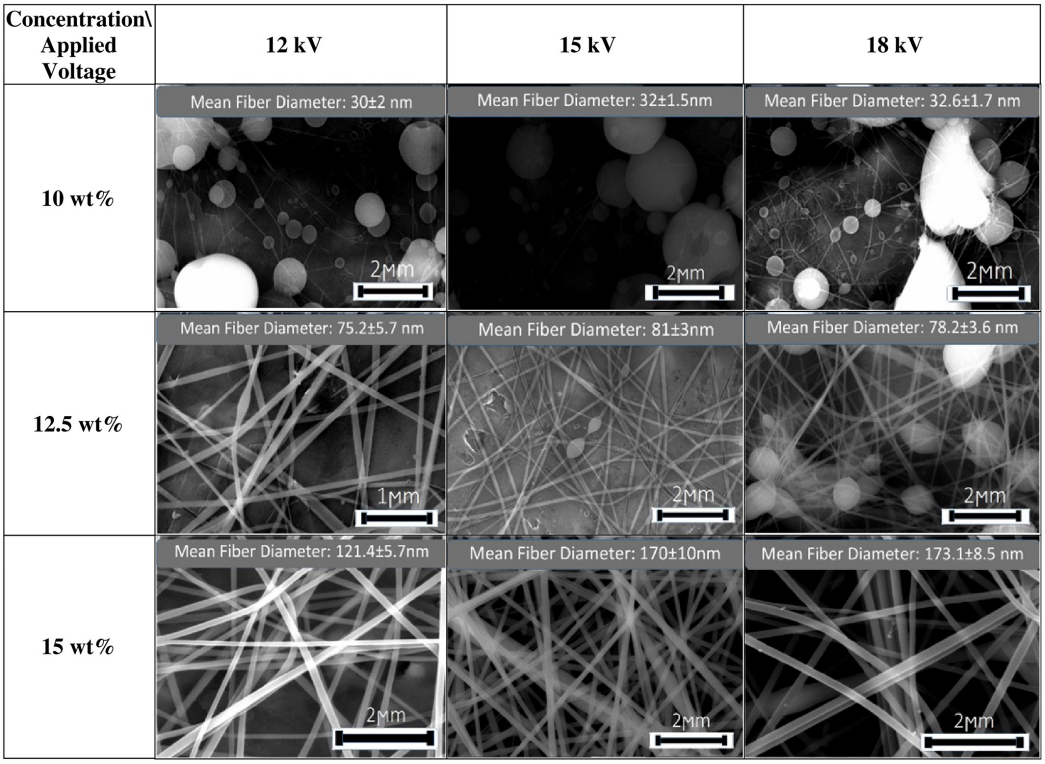


Figure 5. Optimization of PBI nanofibres by varying the polymer concentration and applied voltage at a flow rate of 100 µL/h and a distance of 10 cm. Reprinted with permission from Ref. [27]. 2017, Wiley.

A variety of post-treatments have been examined to enhance the mechanical properties of the PBI nanofibrous membrane [26,28,32]. Chemical treatments are a common way to encourage the crosslinking of polymers after electrospinning. Yu et al. [32] immersed an electrospun PBI mat into a solution of glutaraldehyde to encourage crosslinking and observed how the properties of the nanofibrous mat changed over time. The initial PBI nanofibrous membranes showed smooth and even fibres, free of beading. However, these membranes displayed low mechanical properties (7 MPa of tensile stress at break). The use of glutaraldehyde caused the swelling of the fibre; the diameter increased until 12 h of treatment. After 12 h, the diameter began to decrease again, indicating the occurrence of the crosslinking reactions. The tensile strength of the nanofibrous membranes increased after crosslinking, with significant increases seen up until 24 h of glutaraldehyde treatment (37 MPa of tensile stress at break). However, after this point, the glutaraldehyde bonded to PBI and acted as side-chain plasticizers for the polymer, causing a slight decrease in tensile strength for membranes that had been treated beyond 24 h.

A crosslinking treatment using α,α'-dibromo-m-xylene (DBX) was also performed to improve the chemical and thermal stability of PBI nanofibrous mats for application as a battery separator [28]. In addition, the mats were treated using 4 (chloromethyl) benzoic acid (CMBA) to improve electrolyte wettability. The DBX and CMBA treatments resulted in the formation of rough and curvy nanofibres. In terms of thermal resistance, TGA found weight loss starting as low as 200 °C, but this was likely due to the loss of residual solvent in the fibre. Polymeric weight loss began at around 450 °C. Thermal shrinkage was also measured at 150 °C for 30 min. The membranes displayed excellent thermal resistance at this temperature: no changes in the colour or size of the membrane were observed. The porosity of the PBI membrane was 87% before crosslinking but decreased to 70% following

crosslinking with DBX. However, after CMBA treatment, the porosity increased again to 78%. The mechanical properties of the PBI membrane were also tested, and it was found that after crosslinking, the strength of the membrane increased, but it decreased after the CMBA treatment due to the increase in porosity. At its strongest, the crosslinked membrane had an average tensile strength of 11 mPa. Therefore, this membrane was almost three times weaker than the conventional polyethylene (PE) battery separator, indicating that additional research is needed before the PBI electrospun nanofibrous membrane has the strength to rival the conventional PE membrane.

Physical post-treatments to improve the mechanical properties of PBI nanofibrous membranes have also been tested. Cho et al. [26] used a thermal calendering process and temperatures between 30 and 180 °C to encourage bonding between fibres and increase the strength of the membrane for battery application. As the temperature increased, interbonding between fibres increased, which led to an improvement in the mechanical properties of the nanofibrous membranes. However, this interbonding also led to a decrease in porosity, pore size, and electrolyte uptake as the three-dimensional pore structure was significantly reduced. Moreover, the durability and reusability of PBI membranes for filtration applications were enhanced by laminating the PBI membrane between two layers of polyethylene mesh at 140 °C [30]. This improved the durability by immobilizing the nanofibres and allowing for bend and flex abrasion without significant damage. The membrane was able to be cleaned in acetic acid and deionized water to remove both organic and inorganic compounds, then reused for several cycles.

Other applications of electrospun PBI nanofibres involved post-treatments to improve the specific adsorption or absorption properties of the membrane. One study used molecular imprinting to make the nanofibres selective for the adsorption of sulfonic compounds for application in the oil and gas industry [64]. To obtain the molecular imprint, a small amount of acrylonitrile solution containing sulfone and a dispersant was added to the polymer solution of PBI and lithium bromide salt (LiBr) in DMAc before electrospinning. The adsorption of sulfone was found to be significantly improved after performing the molecular imprinting on the nanofibres. Another study used phosphoric acid (PA)-doped PBI nanofibrous membranes to improve proton conductivity for application as a high-temperature proton exchange membrane [27]. Electrospun PBI membranes were doped in PA for durations of 24, 48, 72, and 96 h, then their conductivity was measured. It was found that a 72 h PA immersion period led to the highest conductivity; at 96 h, free PA in the membrane led to acid leaking. PBI nanofibres have also been used as a substrate for the growth of carbon nanotubes via chemical vapour deposition [66]. The high surface area, porosity, and temperature resistance of the PBI nanofibrous membrane provided an excellent substrate for the carbon nanotubes, producing a nanocomposite suitable for lithium-sulphur batteries and laminated composites.

In summary, PBI nanofibres have been successfully electrospun by a variety of researchers. Currently, there is a major focus on improving the mechanical properties of the membrane using post-treatments such as crosslinking, thermal calendering, and laminating with support materials [26,28,30,32]. Moreover, treatments to improve the thermal properties of the membrane have also been explored to overcome the high thermal shrinkage that is experienced by PBI nanofibrous membranes [28]. Specialized treatments of the PBI nanofibrous membrane have also been used to make the membrane more suitable for specific applications [27,64]. Despite the focus on applications of the studies on PBI nanofibrous membranes, it remains to be determined whether the electrospinning process for PBI can be effectively scaled up. In addition, it will be especially important to consider which post-treatments are most scalable to improve the mechanical and thermal performance of the PBI nanofibrous membranes.

4. Discussion

4.1. State of Progress

The previous section discussed the current progress in the electrospinning of high-performance polymers. Each of the five polymers discussed in this review has experienced progress in electrospinning for the formation of high-performance nanofibrous membranes. However, the stage of progress for each polymer varies considerably. In general, three stages can be observed: (1) the polymer is used in preliminary electrospinning research to determine its viability for nanofibre formation using electrospinning; (2) the electrospinning process for the polymer has been determined, and variations are being made to ensure the nanofibres will share the properties of the corresponding high-performance fibre (e.g., its excellent mechanical properties); (3) the electrospinning and post-treatment of the polymer have been optimized and research is now focused on specific applications and/or industrial scale-up. Depending on the desired application, the second and third progress stages may overlap. For example, a nanofibrous membrane may have the porosity and strength to be applied in a filtration process but lack the necessary chemical stability if chemical resistance is required. Therefore, scale-up may be possible for the less demanding versions of the targeted application before all characteristics of the nanofibre are optimized.

Progress on the electrospinning of p-aramid and PBO nanofibres mainly falls within the first stage, as the viability of electrospinning these polymers is still the major focus of the research at this time. P-aramid has faced considerable challenges in electrospinning due to its high crystallinity, as it can only be dissolved in concentrated sulphuric acid [14]. Likewise, PBO is a rigid-rod polymer and requires concentrated sulphuric acid to form a polymer solution [37,59]. As a result, solution electrospinning is more difficult for these polymers compared to other nanofibre formation processes. For p-aramid, the most promising progress for solution electrospinning is side-chain substitutions on the polymer before electrospinning. This allows p-aramid to be dissolved directly in common organic solvents [3]. However, only one study has looked into this method, and it is still undetermined how side-chain substitutions may impact the properties of the p-aramid nanofibres. Further, the efficiency and scalability of the side-chain substitutions were not discussed in this study. For PBO, more progress has been made in solution electrospinning, with precursors being used to form a polymer solution. Precursors provide a method to produce a polymer solution in an organic solvent, as opposed to a concentrated sulphuric acid solution. Although, the research on electrospinning PBO from precursors is still quite limited [24,25]. When compared to polymers that can be directly dissolved in solvents and electrospun, the processing of PBO nanofibres is more complex, which may not be as favourable for industrial applications. Further, it is uncertain how the post-treatment of the PBO precursor nanofibres could limit the combination with other materials (e.g., coaxial or composite nanofibres). Although research on the electrospinning of PBO predominantly falls within the first stage of electrospinning progress, it is beginning to move toward the second stage, for example with the use of the OH-PAA precursor instead of OH-PA to improve the molecular weight and mechanical strength of the PBO nanofibres [25].

The second stage of electrospinning progress considers polymers for which a viable electrospinning process has been established. In this stage, research is focused on improving the properties of the nanofibres to better align with the expected properties of conventional high-performance fibres. The electrospinning of PBI fits well within this stage. The mechanical strength of PBI nanofibrous membranes has been improved using crosslinking treatments and thermal calendering after electrospinning [26,28,32]. When compared to polymer manipulation before electrospinning, post-treatments may be more easily implemented at an industrial scale. However, crosslinking treatments can adversely affect the resultant nanofibrous membrane, particularly with respect to pore size [32]. Therefore, the ability to improve mechanical properties using both polymer manipulation and post-treatments may be useful in improving the properties of the nanofibrous membranes without affecting the membrane performance. Overall, there is a focus on improving the mechanical properties of high-performance nanofibres as high strength is one of the main

motivations for using these polymers. However, the manipulation of other properties such as chemical resistance, hydrophilicity, hydrophobicity, porosity, and flame resistance has also been attempted for specific applications [21,32,43]. Since these properties are highly dependent on the application, the manipulation of the properties generally does not occur until research has progressed to stage 3, where a direct application is being pursued.

The third stage of research progress covers polymers for which both an electrospinning process and methods to optimize the process and improve the properties of the fibres have been well established. At this stage, research on electrospinning tends to narrow and specify itself to specific applications. Here, researchers may look at variations in membrane orientation, fibre morphology, and physical properties. They may also investigate the use of nanofibres within composites. Within the category of high-performance fibres, m-aramid and PAI are the two polymers best established in electrospinning. Methods for the electrospinning of m-aramid and PAI are well-documented, and the optimization of the electrospinning process has been thoroughly studied; the polymer solution, fibre orientation, and post-treatments of the nanofibrous membranes were considered, among other parameters [9,11,43,45]. Studies to improve the mechanical performance of these nanofibres so that they are closer to the properties of conventional high-performance fibres are ongoing (e.g., via the post-treatment of m-aramid) [45,49]. However, the majority of the research into these fibres considers specific fibre properties for a large number of applications. Examples of electrospinning work with PAI include forming unique fibre morphologies, using it as a support in composite materials, and scaling up the nanofibre manufacturing [19–21]. Likewise, m-aramid is being used within composite materials and has been studied for various applications including surface flame retardants, antimicrobial water filters, lithium-ion batteries, and breathable waterproof membranes [7–9,21,44]. In terms of industrial scalability, nanofibrous PAI has been produced using a needleless electrospinning setup, providing a method for the mass-production of PAI nanofibrous membranes [20]. In contrast, no studies have been conducted that consider the scalability of m-aramid nanofibrous membranes. Future investigation into the use of scalable electrospinning processes, such as needleless or multi-needle electrospinning, will be a vital next step in determining the scalability of m-aramid nanofibres. Although PBI electrospinning progress mainly falls within the second category, specific applications of PBI nanofibrous membranes have been considered, including lithium-ion battery separators, fuel cells, water electrolyzers, respiratory masks, and carbon nanofibre precursors [26,28,30–32]. However, only one study investigated the scale-up processing of PBI using a multinozzle setup [28] and another study produced PBI nanofibrous membranes using a needleless setup [65]. As the applications for PBI move toward mass production, further study of mass production methods becomes necessary. Interestingly, PBI nanofibrous membranes are the only high-performance membranes for which the washing and reuse of the nanofibrous membranes have been examined [30]. Considering that many post-treated nanofibrous membranes become chemically inert and cannot be redissolved, the longevity and reuse of the nanofibrous membranes are important considerations for the supply and value chains of the product. For PAI and m-aramid nanofibrous membranes, exploration of the longevity and reuse potential of the membranes will be important as electrospinning processes move toward industrial scale-up.

Although this review has divided electrospinning progress into three discrete categories, the chronology of the literature does not always reflect the same progression. Specifically, studying the electrospinning of high-performance nanofibres for niche applications often occurs before the optimization of the electrospinning process and/or fibre properties has been well-studied. The major challenge with considering specific applications before basic electrospinning research has been established is that the test methods used to assess the performance of the nanofibres may be highly specific. Moreover, performance results may be compared to material alternatives for a specific application, as opposed to comparison with other nanofibrous membranes. From a production perspective, this limits the understanding of how different electrospinning conditions may affect the outcome of the nanofibrous membrane. More general studies focusing on methods

to improve nanofibre diameter distribution, mechanical strength, or porosity are useful references for several applications. Further, methods to assess the performance of nanofibrous membranes without direct comparison to a material used in a specific application are necessary and useful tools for assessing nanofibrous membrane performance.

4.2. Challenges, Limitations, and Avenues of Solutions

Challenges and limitations have been identified in terms of standardized characterization methods, electrospinning solution preparation, and the mechanical performance of the produced nanofibers. The sections below discuss these challenges and propose potential avenues of solutions.

4.2.1. Standardized Characterization Methods

In general, a major challenge with the study of nanofibres has been the lack of standardized test methods for assessing the performance of the membranes. Since electrospinning is a highly variable process, different research studies have used a wide range of parameters to produce similar nanofibres. This makes a comparison of the outcomes of the electrospinning process between studies very difficult. In addition, the characterization methods of nanofibres are not standardized and the literature varies widely in terms of which characterization methods are used. Visual fibre and web morphologies are generally the easiest to compare within the literature, as most research uses scanning electron microscopy (SEM) and similar image analysis software to determine average fibre diameters and the distributions of fibre diameters and quantify non-fibrous areas. In other instances, the characterization that was performed may not always describe a property in a comprehensive manner. For example, some studies of m-aramid looked at the pore size distribution [10,47]. However, this value is dependent on the thickness of the membrane, which was not always reported. Likewise, studies of chemical changes to the polymer to improve molecular weight or solubility were often reported without the assessment of the effect on mechanical properties [3]. This makes a comparison of different electrospinning and post-treatment methods very difficult. However, such a comparison is necessary to move forward productively in the field. As research on nanofibres continues to grow and standards are published, creating a framework of test methods for characterizing nanofibre performance will be an important tool to increase accuracy and comparability between studies.

The standardized assessment of the mechanical properties of nanofibres continues to be a challenge for nanofibrous membranes due to difficulties in handling the membrane and the extraction of a single nanofibre from the mat without damaging it and the use of load cells outside of their useful range, among others [42]. Table 2 describes test methods typically used to determine the mechanical strengths of high-performance nanofibres. In general, likely due to both the difficulty of extracting a single nanofibre from the membrane and the interest in the overall mechanical properties of the membrane, the entire membrane strength tends to be measured instead of a single fibre. However, the preparation of samples for tensile testing is highly variable between studies. When the membrane is being tested, specimens are typically cut into a rectangular shape or dog-bone shape (Table 2). Some authors also report the use of a paper frame or additional support for the membrane to discourage clamp breakage or damage while mounting the specimen [15,33]. Clamp breakage is a major issue with low-strength material; thus, sample preparation and the use of the correct clamp type are critical to obtain accurate results. The sample preparation procedures used for measuring the strength of high-performance nanofibers have sometimes been adapted from mechanical characterization standards developed for micro-scale materials, for instance, ASTM D638 and ASTM D882. Both methods are intended to assess the mechanical properties of thin plastic sheeting. However, the highly porous structure of nanofibrous membranes compared to plastic sheeting presents some challenges in the applicability of the method, particularly in assessing the overall strength of the membrane [9]. Merighi et al. [43] suggest measuring tensile stress by considering the membrane density in order to account for the high volume of air present in nanofibrous

materials. As the nanofibre alignment and the presence of other additives such as salts can have major impacts on the strength of a nanofibrous membrane, these factors should also be considered when interpreting the results [9].

Table 2. Test methods for assessing the mechanical strength of nanofibres.

Reference	Polymer	Test Method and Specimen Preparation	Equipment	Gauge Length	Stretching Rate	Load Cell
[11]	p-aramid	Single fibre mounted on a test frame of 10 mm × 5 mm using super glue and double-sided tape	Agilent T150-UTM Micro-tensile tester	5 mm	0.1 mm s^{-1}	Minimum resolution of 50 nN
[16]	PAI	Rectangular specimens of nanofibrous mat	CMT-8102 Electromechanical Universal Testing Machine	NR	5 mm/min	NR
[17]	PAI	Not reported	SANS Tensile Testing Machine	NR	5 mm/min	NR
[33]	PBI	ASTM D882-18 Rectangular specimen, 10 mm × 70 mm, thickness of 35–50 µm, foam tape attached at edges to avoid clamp damage	Instron 5442	50 mm	2 mm/min	NR
[26]	PBI	Rectangular specimen of 1 cm × 4 cm	Instron 3433 Universal Testing Machine	NR	50 mm/min	NR
[27]	PBI	ASTM D882-12 Rectangular specimens of 20 mm × 60 mm, thickness of 30 µm	Shimadzu AG-X Plus 100 kN Universal Testing Machine	NR	NR	NR
[32]	PBI	Rectangular specimens of 150 mm × 25 mm	Instron Testing Instrument 4464	100 mm	150 mm/min	NR
[24]	PI-*co*-PBO	Rectangular specimens of aligned nanofibre belts 5 mm × 20 mm	CMT-8102 electromechanical universal testing machine	10 mm	1 mm/min	NR
[43]	m-aramid	Rectangular specimens attached to a paper frame	Remet TC-10	NR	NR	NR
[49]	m-aramid	ASTM D638 Dog-bone-shaped specimens die-cut	Instron 5567 Universal material testing machine	3.18 mm	1 mm/min	NR
[7]	m-aramid	Rectangular specimens of 40 mm × 5 mm	Fangyan YG005 Electronic Single Fiber Strength Tester	NR	10 mm/min	NR
[15]	m-aramid	Rectangular specimens of 20 mm × 50 mm	Kawabata Evaluation System (KES-G1)	NR	100 mm/min	NR
[45]	m-aramid	ASTM D638 Type V Dog-bone-shaped specimens	Instron 3343 Universal testing machine	7.62 mm	1 mm/min	NR
[48]	m-aramid	ASTM D638 Dog-bone-shaped specimens	Instron mechanic static tester	NR	5 mm/min	NR
[47]	m-aramid	Rectangular specimens of 20 mm x 50 mm	Kawabata Evaluation System (KES-G1)	NR	100 mm/min	NR

NR—not reported.

The type of equipment used to assess the strength of nanofibrous membranes presents a second challenge for the characterization of their mechanical performance. A universal tensile testing machine is often used to assess the mechanical strength of nanofibres. However, this equipment is not well adapted to nanomaterials due to the difficulty of mounting a nanofibre onto a test frame. The precision of the load cells also causes the measurements made with universal tensile testing machines to be generally inaccurate for nanofibres with diameters below 100 nm [42]. Some alternatives to the universal mechanical tester have been reported for the mechanical characterization of nanofibrous membranes. For example, the Kawabata Evaluation System (KES) has been used to characterize the mechanical properties of m-aramid nanofibrous membranes [11,47,67]. Moreover, machines designated for testing conventional microfibres have been employed to assess the strength of nanofibrous membranes [7]. The lower load cells on these machines may allow greater accuracy in terms of results. However, a major limitation of measuring the mechanical strength of nanofibres is that this low-force range testing equipment is not as widely available as universal tensile testing machines.

In general, there is a need for testing and analysis methods that consider nanofibrous materials as unique, as opposed to the adaptation of standards intended for plastics. However, since such a standard does not yet exist, reference to other standards can help provide sufficient detail on specimen preparation and testing procedures in an organized manner. The adaptation of an existing standard would also help gain consistency in which test parameters are reported. Key elements of the tensile tests, including ambient conditions, load cell capacity and precision, and test frame configuration are also often omitted from reports of results, making replicability between research groups increasingly difficult. As a result, only comparisons of the mechanical behaviours of fibres and materials produced within a given article are typically possible. The use of a standardized method to assess the mechanical performance of the nanofibres may help gain a more complete understanding of the effects of electrospinning parameters on the mechanical strength of the nanofibres by allowing for a comparison of the strengths of nanofibres produced by various research groups.

The development of standardized test methods for assessing the performance of nanofibrous materials will be necessary to encourage collective progress within the field. Not only will these methods eliminate inconsistencies between studies, but they will also allow for the comparison of performance between high-performance nanofibres. To date, studies on the electrospinning of high-performance nanofibres tend to compare the performance to micro-scale counterparts or to nanofibres electrospun from conventional polymers. Other comparisons between high-performance nanofibres will be a useful tool as the research progresses toward direct applications and industrialization. The shared properties of these fibres such as high strength, heat resistance, and chemical resistance mean that they may have overlaps in terms of applications. However, without a method to compare their performance, the best choice of high-performance polymer may be made based on the ease of electrospinning or the existence of test results for a specific application. Increasing standardization will help decide the most suitable polymer in terms of performance for specific applications.

4.2.2. Dissolution

The dissolution of high-performance fibres continues to be a challenge in electrospinning. The high mechanical properties of these polymers are often associated with a high crystallinity, making their processing difficult [35]. Furthermore, the chemical resistance of the polymers can be considered a major limitation of electrospinning with these polymers, as some are incompatible with common organic solvents. This is especially an issue for p-aramid and PBO, which cannot be directly dissolved in a volatile solvent and must either be modified at the polymer level or spun from a precursor [3,24]. The use of such modifications is helpful in allowing for the electrospinning of these high-performance fibres. However, the complexity of the process may limit industrial implementation. As poly-

mers cannot be bought from manufacturers and directly dissolved, the process becomes increasingly complex.

Other polymers, such as m-aramid, PAI, and PBI, are able to be directly dissolved into organic solvents such as DMAc. They may still require the use of an aprotic salt to encourage dissolution, but it is generally thought to be an effective and simple method to produce a polymer solution [11]. At the lab scale, processes involving organic solvents can be easily controlled to minimize risk. Therefore, the processing of polymers into a solution for electrospinning is a relatively facile procedure that can be easily replicated. At this stage, the majority of high-performance nanofibre electrospinning is occurring in small-scale lab settings. However, the scale-up of electrospinning may become challenging with the use of toxic and flammable solvents, both within the workplace as well as for users who may be exposed to residual solvents within the nanofibres [55]. Industrial scale-up relies largely on needleless electrospinning methods, where the polymer solution may be exposed to air before electrospinning, as opposed to enclosed within a syringe. Large-scale electrospinning equipment is also more difficult to contain within a fume cabinet, which is a common option at the laboratory scale. Therefore, the use of solvents that are highly volatile, toxic, flammable, and/or environmentally harmful is concerning for the scale-up of the production of these nanofibres. When possible, it may be advantageous to consider organic solvents with lower toxicity as solvents for high-performance fibres. In the case of PAI, for example, a variety of organic solvents may be used to dissolve the fibre for electrospinning [54]. Generally, the choice of solvent is made based on the dissolution efficiency and solution properties. However, considering the toxicity, flammability, and environmental impacts of the solvent at an early stage of research may help with later industrial scale-up. Where a toxic solvent is necessary for good dissolution, blending this solvent with a non-toxic or environmentally friendly solvent may be an option to reduce toxicity without compromising solution properties [68].

4.2.3. Mechanical Properties

Another challenge documented in the electrospinning of high-performance nanofibres is the loss in mechanical properties observed when producing fibres at the nanoscale [15]. A drastic decrease in strength is often observed due to poor chain orientation and chain extension within the nanofibres. This is particularly an issue for flexible chain polymers, which have very short relaxation times. Although the jet produced during electrospinning can help orient the polymer, a short relaxation time allows the polymers to relax before solidification on the collector, leading to decreased strength. This issue is also observed in conventional spinning methods and is often remediated with drawing processes to improve polymer alignment. However, at the nanoscale, drawing abilities are increasingly limited and often cannot significantly improve crystallinity or orientation.

In most instances, a direct comparison between the strength of a nanofibre and the strength of a conventional fibre is unavailable, as the majority of research that characterizes the mechanical properties of high-performance nanofibres considers the strength of the overall membrane, as opposed to the strength of a single fibre. One study measured the strength of a single electrospun p-aramid fibre [15]. The 2.1 µm diameter fibre had a tensile strength of approximately 1.0 GPa and a Young's modulus of 58 GPa. A conventional p-aramid fibre typically has a tensile strength greater than 2 MPa and a Young's modulus greater than 60 GPa. In this instance, the strength of the electrospun p-aramid fibre was in the same range as a conventional p-aramid fibre. However, the diameter of the electrospun fibre was not at the nanoscale. Therefore, more data are needed on the mechanical properties of single nanofibres in order to compare their mechanical properties to conventional microfibers.

The mechanical properties of the nanofibre may also be affected by other factors, such as the use of aprotic solvents and salts, which inhibit the recrystallization of the polymer [45]. The use of rigid-rod polymers can improve mechanical strength during electrospinning, as these polymers have a built-in chain extension and can be easily oriented during the

spinning process using elongational flow [15]. Other methods have also been explored to improve the mechanical properties of nanofibres, including strengthening intermolecular interactions from imide groups and hydrogen interactions from amide groups [16].

In terms of the mechanical performance at the membrane level, for non-woven structures, the strength of the membrane is strongly affected by the consolidation of the fibres, as opposed to the inherent strength of the fibres [69,70]. Thus, membrane-level treatments may be more effective at improving the overall strength of the nanofibrous mat. For example, the post-treatment of non-woven membranes is a common option to improve their mechanical strength [69,70]. By joining fibres together within the nanofibrous mat, either by chemical treatment or thermal calendering, for instance, the overall strength of the membrane can be increased [26,28]. However, these treatments typically lead to undesirable side effects including fibre swelling, decreased porosity, increased brittleness, and decreased pore size. Another strategy relies on improving fibre alignment, which increases mat strength in one direction [16]. At the moment, methods to increase the strength of nanofibrous membranes without reducing other membrane properties have not been observed. Moving forward, the use of composites and laminates to improve the durability of nanofibrous membranes where high porosity and low pore size is needed may be a promising path to improve the durability of the membranes [7,30].

4.3. Path Forward

The electrospinning of high-performance polymers continues to be of interest as demand for lightweight porous materials with high strength, chemical resistance, and thermal resistance grows. This review has considered five high-performance polymers and assessed the current progress on the electrospinning of these polymers. For polymers that are difficult to dissolve, such as p-aramid and PBO, more research is needed on effective and efficient electrospinning processes, as well as the characterization and improvement of the nanofibre properties. The research on PBI is progressing but has been limited to characterization for specific applications [28,32]. More general characterization will improve the general understanding of the effect of electrospinning properties on PBI formation, which will be helpful for any application. For PAI, the research has considered a range of production and electrospinning techniques, as well as some applications and scale-up techniques [20,36]. Exploring the use of PAI nanofibres in composites through co-electrospinning or the addition of nanoparticles may be of interest to enhance the nanofibres' properties for specific applications. For m-aramid, there has been good coverage of the optimization of the electrospinning process, the improvement of nanofibre properties, and use in specific applications [9,11,45]. However, no research has considered the scale-up of m-aramid electrospinning. To move the production toward the market, this will be an important next step.

Developing effective methods for the scale-up of electrospinning is a common challenge for the electrospinning of all types of polymers [55]. Needle-based electrospinning has a very low production rate, around 0.01–1 g/h, and is not suitable for mass production. Other techniques, such as multi-jet, multi-needle, and needleless electrospinning provide potential solutions to the issue of low production rates. Currently, only two studies of high-performance polymer electrospinning have considered alternative methods to single-needle electrospinning [20,28]. Although in theory, the principle for these methods is similar to single-needle electrospinning, the parameters of electrospinning must be adjusted to reduce electric field interference, manage changing solution viscosities, and determine different flow rates and electric field strengths that may effectively form fibres with these alternative electrospinning setups. The comparison of various high-production electrospinning methods to achieve the most efficient and precise electrospinning process for high-performance fibres will be an important next step as electrospun high-performance nanofibres move toward the market. Furthermore, as scale-up and the industrial production of nanofibres are considered, the need for standardized characterization methods to assess nanofibrous membranes increases. These methods will help to ensure that scale-up electrospinning

processes are producing similar results to lab-based electrospinning processes. Moreover, the standardized characterization will help to ease the adoption of nanofibrous materials into existing standards for various applications, as the nanofibrous membrane performance can be accurately compared to conventional materials that may be used for the same applications.

The current stage of progress within the electrospinning of high-performance nanofibres positions each polymer at a different level of development. At this stage, before any of the nanofibres reach mass market production, it is critical to compare the different types of high-performance nanofibres in order to find the best fit for each specific application. Generally, high-performance polymers are used for their high strength and thermal resistance. Since these are commonalities among all the nanofibres explored in this review, other factors such as the ease of electrospinning and cost may be important considerations in the applications of the nanofibres. The long-term performance of high-performance nanofibres should also be considered as the research progresses. Mechanical tests are typical for assessing the probability of the premature failure of nanofibres [42]. However, other factors that may degrade the nanofibres during specific applications such as ultraviolet light, cleaning processes, exposure to moisture, exposure to chemicals, and abrasion should be considered to determine the expected lifetime of these nanofibrous membranes. Where the nanofibrous membrane's lifetime is found to be shorter than the required lifetime of the product, replacement and maintenance procedures should also be considered. Finally, end-of-life and recycling procedures for the nanofibrous membranes should be considered in order to mitigate the environmental impact of the membranes [30,71].

5. Conclusions

This review has summarized the current state of electrospinning research for five high-performance fibres: meta-aramid, para-aramid, PAI, PBO, and PBI. P-aramid and PBO are insoluble in common solvents, thus the electrospinning process is more difficult. However, alternative methods for electrospinning have been found for producing polymer solutions for electrospinning using side-chain modification and precursors. PAI, m-aramid, and PBI are more easily soluble in organic solvents. These polymers are largely electrospun as-is and the properties of the nanofibres have been successfully improved using post-treatments. Nanofibres with excellent mechanical properties and thermal resistance continue to be of interest for various applications. Therefore, gaining an understanding of the state of electrospinning research for high-performance polymers is critical for understanding the best path forward.

The ease of solubility remains a challenge and will have to be solved in order to move toward industrialization, hopefully in the coming years. It will be important that the solutions developed have no adverse effects on the performance of the electrospun membranes. As the research transitions to mass production, the issues with scale-up, solvent usage, and end-of-life as well as the need for standardized testing will come to the forefront. Determining methods to select the best material for the nanofibres for a particular application and characterization methods to assess the useful lifetime of the membranes will be a critical next step to be able to take advantage of the unique opportunities offered by electrospun high-performance fibres for highly technical applications.

Author Contributions: Conceptualization, J.R.P.F., F.L. and P.I.D.; methodology, J.R.P.F.; investigation, J.R.P.F.; resources, F.L., E.D. and P.I.D.; data curation, J.R.P.F.; writing—original draft preparation, J.R.P.F.; writing—review and editing, F.L., E.D. and P.I.D.; visualization, J.R.P.F.; supervision, F.L., E.D. and P.I.D.; funding acquisition, J.R.P.F. and P.I.D. All authors have read and agreed to the published version of the manuscript.

Funding: Financial support for conducting this research was provided by the Natural Sciences and Engineering Research Council of Canada (NSERC).

Data Availability Statement: Data of reported tests performed by the authors are available from the corresponding author upon reasonable request. For the other results mentioned, data are available in the articles cited.

Acknowledgments: The authors would like to thank Saiful Hoque for his help in producing the SEM image of the m-aramid nanofibres.

Conflicts of Interest: The authors declare no conflict of interest.

References

1. Bourbigot, S.; Flambard, X. Heat Resistance and Flammability of High Performance Fibres: A Review. *Fire Mater.* **2002**, *26*, 155–168. [CrossRef]
2. Ramakrishna, S.; Fujihara, K.; Teo, W.-E.; Lim, T.-C.; Ma, Z. An Introduction to Electrospinning and Nanofibres. World Scientific: Singapore, 2005.
3. Yeager, M.P.; Hoffman, C.M., Jr.; Xia, Z.; Trexler, M.M. Method for the Synthesis of Para-Aramid Nanofibers. *J. Appl. Polym. Sci.* **2016**, *133*, 1–8. [CrossRef]
4. Babar, A.A.; Iqbal, N.; Wang, X.; Yu, J.; Ding, B. Chapter 1—Introduction and Historical Overview. In *Electrospinning: Nanofabrication and Applications*; Ding, B., Wang, X., Yu, J., Eds.; Micro and Nano Technologies; William Andrew Publishing: Amsterdam, The Netherlands, 2019; pp. 3–20. ISBN 978-0-323-51270-1.
5. Jang, W.G.; Jeon, K.S.; Byun, H.S. The Preparation of Porous Polyamide-Imide Nanofiber Membrane by Using Electrospinning for MF Application. *Desalin. Water Treat.* **2013**, *51*, 5283–5288. [CrossRef]
6. Yu, J.; Qiu, Y.; Zha, X.; Yu, M.; Yu, J.; Rafique, J.; Yin, J. Production of Aligned Helical Polymer Nanofibers by Electrospinning. *Eur. Polym. J.* **2008**, *44*, 2838–2844. [CrossRef]
7. Li, Y.; Ma, X.; Deng, N.; Kang, W.; Zhao, H.; Li, Z.; Cheng, B. Electrospun SiO2/PMIA Nanofiber Membranes with Higher Ionic Conductivity for High Temperature Resistance Lithium-Ion Batteries. *Fibers Polym.* **2017**, *18*, 212–220. [CrossRef]
8. Kim, S.S.; Jung, D.; Choi, U.H.; Lee, J. Antimicrobial *m* -Aramid Nanofibrous Membrane for Nonpressure Driven Filtration. *Ind. Eng. Chem. Res.* **2011**, *50*, 8693–8697. [CrossRef]
9. Mazzocchetti, L.; Benelli, T.; Maccaferri, E.; Merighi, S.; Belcari, J.; Zucchelli, A.; Giorgini, L. Poly-m-Aramid Electrospun Nanofibrous Mats as High-Performance Flame Retardants for Carbon Fiber Reinforced Composites. *Compos. Part B Eng.* **2018**, *145*, 252–260. [CrossRef]
10. Park, Y.S.; Lee, J.W.; Nam, Y.S.; Park, W.H. Breathable Properties of M-Aramid Nanofibrous Membrane with High Thermal Resistance. *J. Appl. Polym. Sci.* **2015**, *132*, 1–6. [CrossRef]
11. Yao, L.; Lee, C.; Kim, J. Fabrication of Electrospun Meta-Aramid Nanofibers in Different Solvent Systems. *Fibers Polym.* **2010**, *11*, 1032–1040. [CrossRef]
12. Yu, J.; Kim, Y.-G.; Kim, D.Y.; Lee, S.; Joh, H.-I.; Jo, S.M. Super High Flux Microfiltration Based on Electrospun Nanofibrous M-Aramid Membranes for Water Treatment. *Macromol. Res.* **2015**, *23*, 601–606. [CrossRef]
13. Gonzalez, G.M.; MacQueen, L.A.; Lind, J.U.; Fitzgibbons, S.A.; Chantre, C.O.; Huggler, I.; Golecki, H.M.; Goss, J.A.; Parker, K.K. Production of Synthetic, Para-Aramid and Biopolymer Nanofibers by Immersion Rotary Jet-Spinning. *Macromol. Mater. Eng.* **2017**, *302*, 1600365. [CrossRef]
14. Yang, B.; Wang, L.; Zhang, M.; Luo, J.; Lu, Z.; Ding, X. Fabrication, Applications, and Prospects of Aramid Nanofiber. *Adv. Funct. Mater.* **2020**, *30*, 2000186. [CrossRef]
15. Yao, J.; Jin, J.; Lepore, E.; Pugno, N.M.; Bastiaansen, C.W.M.; Peijs, T. Electrospinning of P-Aramid Fibers. *Macromol. Mater. Eng.* **2015**, *300*, 1238–1245. [CrossRef]
16. Duan, G.; Liu, S.; Jiang, S.; Hou, H. High-Performance Polyamide-Imide Films and Electrospun Aligned Nanofibers from an Amide-Containing Diamine. *J. Mater. Sci.* **2019**, *54*, 6719–6727. [CrossRef]
17. Feng, Y.; Xiong, T.; Xu, H.; Li, C.; Hou, H. Polyamide-Imide Reinforced Polytetrafluoroethylene Nanofiber Membranes with Enhanced Mechanical Properties and Thermal Stabilities. *Mater. Lett.* **2016**, *182*, 59–62. [CrossRef]
18. Heo, G.; Hong, Y.; Park, S. Preparation and Characterization of Nickel-Coated Carbon Nanofibers Produced from the Electropsinning of Polyamideimide Precursor. *Macromol. Res.* **2012**, *20*, 503–507. [CrossRef]
19. Hua, Y.; Li, Y.; Ji, Z.; Cui, W.; Wu, Z.; Fan, J.; Liu, Y. Dual-Bionic, Fluffy, and Flame Resistant Polyamide-Imide Ultrafine Fibers for High-Temperature Air Filtration. *Chem. Eng. J.* **2023**, *452*, 139168. [CrossRef]
20. Oertel, A.; Nabyl, K.; Laurence, S.; Dominique, C.A.; Hélène, G. Optimization of Meta-Aramid Electrospun Nanofibers Productivity through Wire-Based Electrospinning Setup Scale Up. *J. Ind. Text.* **2018**, *48*, 236–254. [CrossRef]
21. Park, S.-J.; Yop Rhee, K.; Jin, F.-L. Improvement of Hydrophilic Properties of Electrospun Polyamide-Imide Fibrous Mats by Atmospheric-Pressure Plasma Treatment. *J. Phys. Chem. Solids* **2015**, *78*, 53–58. [CrossRef]
22. Hao, R.R.; Jin, J.H.; Yang, S.L. Preparation and Properties of MWCNTs/ PBO Membrane by Electrospinning. *Appl. Mech. Mater.* **2014**, *577*, 58–61. [CrossRef]
23. Hsu, S.L.-C.; Lin, K.-S.; Wang, C. Preparation of Polybenzoxazole Fibers via Electrospinning and Postspun Thermal Cyclization of Polyhydroxyamide. *J. Polym. Sci. Part A Polym. Chem.* **2008**, *46*, 8159–8169. [CrossRef]

24. Jiang, S.; Duan, G.; Chen, L.; Hu, X.; Ding, Y.; Jiang, C.; Hou, H. Thermal, Mechanical and Thermomechanical Properties of Tough Electrospun Poly(Imide- Co -Benzoxazole) Nanofiber Belts. *New J. Chem.* **2015**, *39*, 7797–7804. [CrossRef]
25. Zhang, H.; Jiang, S.; Duan, G.; Li, J.; Liu, K.; Zhou, C.; Hou, H. Heat-Resistant Polybenzoxazole Nanofibers Made by Electrospinning. *Eur. Polym. J.* **2014**, *50*, 61–68. [CrossRef]
26. Cho, S.J.; Choi, H.; Youk, J.H. Evaluation of PBI Nanofiber Membranes as a High-Temperature Resistance Separator for Lithium-Ion Batteries. *Fibers Polym.* **2020**, *21*, 993–998. [CrossRef]
27. Jahangiri, S.; Aravi, İ.; Işıkel Şanlı, L.; Menceloğlu, Y.Z.; Özden-Yenigün, E. Fabrication and Optimization of Proton Conductive Polybenzimidazole Electrospun Nanofiber Membranes. *Polym. Adv. Technol.* **2018**, *29*, 594–602. [CrossRef]
28. Jung, J.H.; Vijayakumar, V.; Haridas, A.K.; Ahn, J.-H.; Nam, S.Y. Effect of Cross-Linking and Surface Treatment on the Functional Properties of Electrospun Polybenzimidazole Separators for Lithium Metal Batteries. *ACS Omega* **2022**, *7*, 47784–47795. [CrossRef] [PubMed]
29. Kim, T.-K.; Choi, K.-Y.; Lee, K.-S.; Park, D.-W.; Jin, M.Y. Thermal Conversion of T-Butyloxycarbonyloxy Attached Polyamides to Polybenzoxazoles. *Polym. Bull.* **2000**, *44*, 55–62. [CrossRef]
30. Lee, S.; Cho, A.R.; Park, D.; Kim, J.K.; Han, K.S.; Yoon, I.-J.; Lee, M.H.; Nah, J. Reusable Polybenzimidazole Nanofiber Membrane Filter for Highly Breathable PM2.5 Dust Proof Mask. *ACS Appl. Mater. Interfaces* **2019**, *11*, 2750–2757. [CrossRef]
31. Najibah, M.; Tsoy, E.; Khalid, H.; Chen, Y.; Li, Q.; Bae, C.; Hnát, J.; Plevová, M.; Bouzek, K.; Jang, J.H.; et al. PBI Nanofiber Mat-Reinforced Anion Exchange Membranes with Covalently Linked Interfaces for Use in Water Electrolysers. *J. Membr. Sci.* **2021**, *640*, 119832. [CrossRef]
32. Yu, T.-L.L.; Liu, S.-H.; Lin, H.-L.; Su, P.-H. Nafion/PBI Nanofiber Composite Membranes for Fuel Cells Applications. In Proceedings of the ASME 2010 8th International Fuel Cell Science, Engineering and Technology, Brooklyn, NY, USA, 14–16 June 2010; ASMEDC: Brooklyn, NY, USA, 2010; Volume 2, pp. 631–639.
33. Zholobko, O.; Wu, X.-F.; Zhou, Z.; Aulich, T.; Thakare, J.; Hurley, J. A Comparative Experimental Study of the Hygroscopic and Mechanical Behaviors of Electrospun Nanofiber Membranes and Solution-Cast Films of Polybenzimidazole. *J. Appl. Polym. Sci.* **2020**, *137*, 49639. [CrossRef]
34. Fan, Y.; Li, Z.; Wei, J. Application of Aramid Nanofibers in Nanocomposites: A Brief Review. *Polymers* **2021**, *13*, 3071. [CrossRef] [PubMed]
35. Zhang, B.; Wang, W.; Tian, M.; Ning, N.; Zhang, L. Preparation of Aramid Nanofiber and Its Application in Polymer Reinforcement: A Review. *Eur. Polym. J.* **2020**, *139*, 109996. [CrossRef]
36. Ding, Y.; Hou, H.; Zhao, Y.; Zhu, Z.; Fong, H. Electrospun Polyimide Nanofibers and Their Applications. *Prog. Polym. Sci.* **2016**, *61*, 67–103. [CrossRef]
37. Reneker, D.H.; Chun, I. Nanometre Diameter Fibres of Polymer, Produced by Electrospinning. *Nanotechnology* **1996**, *7*, 216. [CrossRef]
38. Long, Y.-Z.; Yan, X.; Wang, X.-X.; Zhang, J.; Yu, M. Chapter 2—Electrospinning: The Setup and Procedure. In *Electrospinning: Nanofabrication and Applications*; Ding, B., Wang, X., Yu, J., Eds.; Micro and Nano Technologies; William Andrew Publishing: Amsterdam, The Netherlands, 2019; pp. 21–52. ISBN 978-0-323-51270-1.
39. Ramakrishna, S.; Fujihara, K.; Teo, W.-E.; Lim, T.-C.; Ma, Z. Solution Property. In *An Introduction to Electrospinning and Nanofibres*; World Scientific: Singapore, 2005; pp. 63–80.
40. Taylor, G.I.; Van Dyke, M.D. Electrically Driven Jets. *Proc. R. Soc. Lond. A Math. Phys. Sci.* **1969**, *313*, 453–475. [CrossRef]
41. Li, Z.; Wang, C. Effects of Working Parameters on Electrospinning. In *One-Dimensional Nanostructures: Electrospinning Technique and Unique Nanofibers*; Li, Z., Wang, C., Eds.; SpringerBriefs in Materials; Springer: Berlin/Heidelberg, Germany, 2013; pp. 15–28. ISBN 978-3-642-36427-3.
42. Tan, E.P.S.; Lim, C.T. Mechanical Characterization of Nanofibers—A Review. *Compos. Sci. Technol.* **2006**, *66*, 1102–1111. [CrossRef]
43. Merighi, S.; Mazzocchetti, L.; Benelli, T.; Maccaferri, E.; Zucchelli, A.; D'Amore, A.; Giorgini, L. A New Wood Surface Flame-Retardant Based on Poly-m-Aramid Electrospun Nanofibers. *Polym. Eng. Sci.* **2019**, *59*, 2541–2549. [CrossRef]
44. Merighi, S.; Maccaferri, E.; Belcari, J.; Zucchelli, A.; Benelli, T.; Giorgini, L.; Mazzocchetti, L. Interaction between Polyaramidic Electrospun Nanofibers and Epoxy Resin for Composite Materials Reinforcement. *Key Eng. Mater.* **2017**, *748*, 39–44. [CrossRef]
45. Chung, J.; Kwak, S.-Y. Solvent-Assisted Heat Treatment for Enhanced Chemical Stability and Mechanical Strength of Meta-Aramid Nanofibers. *Eur. Polym. J.* **2018**, *107*, 46–53. [CrossRef]
46. Wu, H.; Bian, F.; Gong, R.H.; Zeng, Y. Effects of Electric Field and Polymer Structure on the Formation of Helical Nanofibers via Coelectrospinning. *Ind. Eng. Chem. Res.* **2015**, *54*, 9585–9590. [CrossRef]
47. Yao, L.R.; Kim, J.Y. The Microstructure and Mechanical Property of Meta-Aramid Nanofiber Web for High Temperature Filter Media. *Adv. Mater. Res.* **2011**, *175–176*, 318–322. [CrossRef]
48. Oh, H.J.; Pant, H.R.; Kang, Y.S.; Jeon, K.S.; Pant, B.; Kim, C.S.; Kim, H.Y. Synthesis and Characterization of Spider-Web-like Electrospun Mats of Meta-Aramid. *Polym. Int.* **2012**, *61*, 1675–1682. [CrossRef]
49. Oh, H.J.; Han, S.H.; Kim, S.S. A Novel Method for a High-Strength Electrospun Meta-Aramid Nanofiber by Microwave Treatment. *J. Polym. Sci. Part B Polym. Phys.* **2014**, *52*, 807–814. [CrossRef]
50. Tian, X.; Zhang, F.; Xin, B.; Liu, Y.; Gao, W.; Wang, C.; Zheng, Y. Electrospun Meta-Aramid/Polysulfone-Amide Nanocomposite Membranes for the Filtration of Industrial PM2.5 Particles. *Nanotechnology* **2019**, *31*, 055702. [CrossRef]

51. Jin, S.; Xin, B.; Zheng, Y. Preparation and Characterization of Polysulfone Amide Nanoyarns by the Dynamic Rotating Electrospinning Method. *Text. Res. J.* **2019**, *89*, 52–62. [CrossRef]
52. Koo, K.; Park, Y.M.; Choe, J.D.; Kim, E.A. Preparations of Microencapsulated PCMs-Coated Nylon Fabrics by Wet and Dry Coating Process and Comparison of Their Properties. *Polym. Eng. Sci.* **2009**, *49*, 1151–1157. [CrossRef]
53. Guo, Y.; Tian, Q.; Wang, T.; Wang, S.; He, X.; Ji, L. Silver Nanoparticles Decorated Meta-Aramid Nanofibrous Membrane with Advantageous Properties for High-Performance Flexible Pressure Sensor. *J. Colloid Interface Sci.* **2023**, *629*, 535–545. [CrossRef]
54. Liaw, D.-J.; Liaw, B.-Y. Synthesis and Characterization of New Polyamide-Imides Containing Pendent Adamantyl Groups. *Polymer* **2001**, *42*, 839–845. [CrossRef]
55. Omer, S.; Forgách, L.; Zelkó, R.; Sebe, I. Scale-up of Electrospinning: Market Overview of Products and Devices for Pharmaceutical and Biomedical Purposes. *Pharmaceutics* **2021**, *13*, 286. [CrossRef] [PubMed]
56. Elmarco NS 1S500U Electrospinning Machine. Available online: https://www.elmarco.com//production-lines/ns-1s500u (accessed on 16 December 2022).
57. Srinivasan, G.; Reneker, D.H. Structure and Morphology of Small Diameter Electrospun Aramid Fibers. *Polym. Int.* **1995**, *36*, 195–201. [CrossRef]
58. Cao, K.; Siepermann, C.P.; Yang, M.; Waas, A.M.; Kotov, N.A.; Thouless, M.D.; Arruda, E.M. Reactive Aramid Nanostructures as High-Performance Polymeric Building Blocks for Advanced Composites. *Adv. Funct. Mater.* **2013**, *23*, 2072–2080. [CrossRef]
59. Duan, G.; Jiang, S.; Chen, S.; Hou, H. Heat and Solvent Resistant Electrospun Polybenzoxazole Nanofibers from Methoxy-Containing Polyaramide. *J. Nanomater.* **2010**, *2010*, 1–5. [CrossRef]
60. Tullos, G.L.; Powers, J.M.; Jeskey, S.J.; Mathias, L.J. Thermal Conversion of Hydroxy-Containing Imides to Benzoxazoles: Polymer and Model Compound Study. *Macromolecules* **1999**, *32*, 3598–3612. [CrossRef]
61. Tullos, G.L.; Mathias, L.J. Unexpected Thermal Conversion of Hydroxy-Containing Polyimides to Polybenzoxazoles. *Polymer* **1999**, *40*, 3463–3468. [CrossRef]
62. Vogel, H.; Marvel, C.S. Polybenzimidazoles, New Thermally Stable Polymers. *J. Polym. Sci.* **1961**, *50*, 511–539. [CrossRef]
63. Kim, J.-S.; Reneker, D.H. Polybenzimidazole Nanofiber Produced by Electrospinning. *Polym. Eng. Sci.* **1999**, *39*, 849–854. [CrossRef]
64. Ogunlaja, A.S.; du Sautoy, C.; Torto, N.; Tshentu, Z.R. Design, Fabrication and Evaluation of Intelligent Sulfone-Selective Polybenzimidazole Nanofibers. *Talanta* **2014**, *126*, 61–72. [CrossRef]
65. Ponomarev, I.I.; Skupov, K.M.; Modestov, A.D.; Lysova, A.A.; Ponomarev, I.I.; Vtyurina, E.S. Cardo Polybenzimidazole (PBI-O-PhT) Based Membrane Reinforced with m-Polybenzimidazole Electrospun Nanofiber Mat for HT-PEM Fuel Cell Applications. *Membranes* **2022**, *12*, 956. [CrossRef]
66. Yildiz, K.; Alrai, A.; Erturk, M.; Koken, D.; Bozali, B.; Zakaria, A.Z.; Cebeci, F.C.; Ozden-Yenigun, E.; Cebeci, H. Morphology-Property Relationship in Radially Oriented Anchored Carbon Nanotubes on Polybenzimidazole Nanofibers. *J. Mater. Sci.* **2023**, *58*, 9978–9990. [CrossRef]
67. Kawabata, S.; Niwa, M. Fabric Performance in Clothing and Clothing Manufacture. *J. Text. Inst.* **1989**, *80*, 19–50. [CrossRef]
68. Alqaheem, Y.; Alomair, A.A. Minimizing Solvent Toxicity in Preparation of Polymeric Membranes for Gas Separation. *ACS Omega* **2020**, *5*, 6330–6335. [CrossRef] [PubMed]
69. Wang, Y. Effect of Consolidation Method on the Mechanical Properties of Nonwoven Fabric Reinforced Composites. *Appl. Compos. Mater.* **1999**, *6*, 19–34. [CrossRef]
70. Yilmaz, K.B.; Sabuncuoglu, B.; Yildirim, B.; Silberschmidt, V.V. A Brief Review on the Mechanical Behavior of Nonwoven Fabrics. *J. Eng. Fibers Fabr.* **2020**, *15*, 1558925020970197. [CrossRef]
71. Shu, R.; Zhang, Q.; Zhao, Y.-B.; Lv, C.; Liu, J.; Wang, J. An Efficient Method to Recycle and Reuse Meta-Aramid from Used Dust Filter Bags. *Sep. Purif. Technol.* **2022**, *299*, 121692. [CrossRef]

Disclaimer/Publisher's Note: The statements, opinions and data contained in all publications are solely those of the individual author(s) and contributor(s) and not of MDPI and/or the editor(s). MDPI and/or the editor(s) disclaim responsibility for any injury to people or property resulting from any ideas, methods, instructions or products referred to in the content.